INSTITUTO SUPERIOR DE ENGENHARIA DO PORTO
MESTRADO EM ENGENHARIA ELECTROTÉCNICA E DE COMPUTADORES

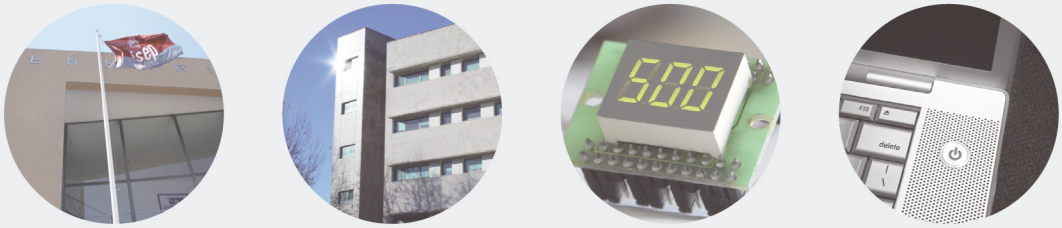

Virtual Reality Applied to Welder Training

MANUEL BENTO BARBOSA DO COUTO
outubro de 2023

POLITÉCNICO
DO PORTO

Politécnico do Porto
Instituto Superior de Engenharia do Porto

Virtual Reality Applied to Welder Training

Manuel Bento Barbosa do Couto

Master in Electrical and Computer Engineering
Specialization Area of Automation and Systems

Departamento de Engenharia Eletrotécnica
Instituto Superior de Engenharia do Porto

October, 2023

This dissertation partially satisfies the requirements of the Thesis/Dissertation course of the program Master in Electrical and Computer Engineering, Specialization Area of Automation and Systems.

Candidate: Manuel Bento Barbosa do Couto, No. 1181160, 1181160@isep.ipp.pt

Scientific Guidance: Manuel Fernando dos Santos Silva, mss@isep.ipp.pt

Company: INESC TEC - Institute for Systems and Computer Engineering, Technology and Science

Advisor: Marcelo R. Petry, marcelo.petry@inesctec.pt

Departamento de Engenharia Eletrotécnica
Instituto Superior de Engenharia do Porto
Rua Dr. António Bernardino de Almeida, 431, 4200–072 Porto

October, 2023

Acknowledgements

I would like to extend my sincere gratitude to the following individuals and institutions who have played a pivotal role in my academic journey and the completion of this thesis.

First and foremost, I express my heartfelt appreciation to the Instituto Superior de Engenharia do Porto (ISEP), my academic home for the past five years. The knowledge and skills I acquired during my time at ISEP have been instrumental in shaping my academic and professional growth.

I would like to acknowledge the Institute for Systems and Computer Engineering, Technology, and Science (INESC TEC) for providing me with the opportunity to undertake my research project under their guidance. The support and resources offered by INESC TEC have been invaluable in the development and execution of my research.

I owe a debt of gratitude to my esteemed advisors, Professor Manuel Silva and Professor Marcelo Petry, for their unwavering support, invaluable guidance, and scholarly expertise. Their mentorship has been instrumental in shaping the direction and quality of this work.

Additionally, I want to express my heartfelt thanks to my family and friends who have been a constant source of encouragement and support throughout this journey. Special appreciation goes to Stéphane Oliveira, Augusto Ulisses, João Fonseca, João Dias, Stéphane Monteiro, Diogo Freitas, and Ismael Costa for their camaraderie and unwavering support during my Master's program.

To all those mentioned above and countless others who have contributed to my academic and personal growth, thank you.

Abstract

Welding is a challenging, risky, and time-consuming profession. Recently, there has been a documented shortage of trained welders, and as a result, the market is pushing for an increase in the rate at which new professionals are trained. To address this growing demand, training institutions are exploring alternative methods to train future professionals with the goals of improving learner retention of information, shortening training periods, and lowering associated expenses. The emergence of virtual reality technologies has led to initiatives to explore their potential for welding training. Multiple studies have suggested that virtual reality training delivers comparable, or even superior, results when compared to more conventional approaches, with shorter training times and reduced costs in consumables. Additionally, virtual reality allows trainees to try out different approaches to their work. The primary goal of this dissertation is to develop a virtual reality welding simulator. To achieve this objective effectively, the creation of a classification system capable of identifying the simulator's key characteristics becomes imperative. Therefore, the secondary objective of this thesis is to develop a classification system for the accurate evaluation and comparison of virtual reality welding simulators.

Regarding the virtual reality welding simulation, the HTC VIVE Pro 2 virtual reality equipment was employed, to transfer the user's action from the physical to the virtual world. Within this virtual environment, it was introduced a suite of welding tools and integrated a Smoothed Particle Hydrodynamics simulator to mimic the weld creation. After conducting comprehensive testing that revealed certain limitations in welding quality and in the simulator performance, the project opted to incorporate a Computational Fluid Dynamics (CFD) simulator. The development of the CFD simulator proved to be a formidable challenge, and regrettably, its complete implementation was unattainable. Nevertheless, the project delved into three distinct grid architectures, from these, the dynamic grid was ultimately implemented. It also proficiently integrated two crucial solvers for the Navier-Stokes equations. These functions were implemented in the Graphics Processing Unit (GPU), to improve their efficiency. Upon comparing GPU and Central Processing Unit (CPU) performance, the project highlighted the substantial computational advantages of

GPUs and the advantages it brings to fluid simulations.

Keywords: welding, training, education, virtual reality, augmented reality, simulation, smoothed particle hydrodynamics, computational fluid dynamics, Navier-Stokes equations.

Resumo

A soldadura é uma profissão exigente, perigosa e que requer um grande investimento de tempo para alcançar resultados satisfatórios. Recentemente, tem sido registada uma falta de profissionais qualificados na área da soldadura. Como resultado, o mercado está a pressionar para um aumento do ritmo a que os novos trabalhadores são formados. Para responder a esta crescente procura, as instituições de formação estão a explorar métodos alternativos para formar futuros profissionais, com o objetivo de melhorar a retenção de informação, encurtar os períodos de treino e reduzir as despesas associadas. Com o desenvolvimento de tecnologias nas áreas de realidade virtual e realidade aumentada, têm surgido iniciativas para explorar o potencial destas na formação de soldadura. Vários estudos sugeriram que a formação em realidade virtual proporciona resultados comparáveis, ou mesmo superiores, aos de abordagens mais convencionais, com tempos de formação mais curtos e reduções nos custos de consumíveis. Além disso, a realidade virtual permite aos formandos experimentar diferentes abordagens ao seu trabalho. O objetivo principal desta dissertação é o desenvolvimento de um simulador de soldadura em realidade virtual. Para atingir este objetivo de forma eficaz, torna-se imperativa a criação de um sistema de classificação capaz de identificar as características chave do simulador. Assim, o objetivo secundário desta dissertação é desenvolver um sistema de classificação para a avaliação e comparação precisas de simuladores de soldadura em realidade virtual.

Relativamente ao simulador de soldadura em realidade virtual, foi utilizado o kit de realidade virtual HTC VIVE Pro 2, para transferir as ações do utilizador no mundo físico para o mundo virtual. No ambiente virtual, foi introduzido um conjunto de ferramentas de soldadura e integrado um simulador de Hidrodinâmica de Partículas Suavizadas para simular a criação da solda. Após a realização de testes exaustivos que revelaram algumas limitações na qualidade da solda e no desempenho do simulador, o projeto optou por incorporar um simulador de Dinâmica de Fluidos Computacional (CFD). O desenvolvimento do simulador CFD revelou-se um desafio formidável e, infelizmente, não foi possivel completar a sua implementação. No entanto, o projeto aprofundou três arquitecturas de grelha distintas, das quais foi implementada a grelha dinâmica. O projeto também implementou duas funções cruciais para resolver as equações de Navier-Stokes. As funções relativas ao simulador de fluidos foram implementadas na Unidade de Processamento Gráfico (GPU), a fim de melhorar a sua eficiência. Ao comparar o desempenho da GPU com o da Unidade

Central de Processamento (CPU), o projeto evidenciou os beneficios computacionais das GPUs e as vantagens que trazem para as simulações de fluidos.

Palavras-Chave: soldadura, formação, educação, realidade virtual, realidade aumentada, simulador, hidrodinâmica de partículas suavizadas, dinâmica de fluidos computacional, equações de Navier-Stokes.

Contents

List of Figures

List of Tables

List of Acronyms

2D	Two-Dimensional
3D	Three-Dimensional
ANSI	American National Standards Institute
AR	Augmented Reality
AWS	American Welding Society
CFD	Computational Fluid Dynamics
CO_2	Carbon Dioxide
CPU	Central Processing Unit
CTWD	Contact to Work Distance
FCAW	Flux-Cored Arc Welding
FOV	Field of View
FPS	Frames Per Second
GMAW	Gas Metal Arc Welding
GPU	Graphics Processing Unit
GTAW	Gas Tungsten Arc Welding
HLSL	High-Level Shader Language
HMD	Head Mounted Display
HSE	Health and Safety Executive
ICL	International Conference on Interactive Collaborative Learning
INESC TEC	Institute for Systems and Computer Engineering, Technology and Science
ISO	International Organization for Standardization

LBM	Lattice Boltzmann Method
MAG	Metal Active Gas
MIG	Metal Inert Gas
SAW	Submerged Arc Welding
SMAW	Shielded Metal Arc Welding
SPH	Smoothed-Particle Hydrodynamics
TIG	Tungsten Inert Gas
VR	Virtual Reality
VRWS	Virtual Reality Welding Simulator
XR	Extended Reality

Chapter 1

Introduction

Welding is not a recent activity, in fact, it has been around for thousands of years, and it can be traced back to the Bronze Age. Since then, it has evolved and changed drastically. Initially, welding was achieved by hammering metals together, this process is known as diffusion bonding, in which the metals undergo a microscopic deformation, and the joint region becomes homogeneous [1]. This process was used to create weapons, tools, and household items. During the Iron Age, blacksmiths developed new techniques for forge welding, including the use of fluxes to protect the metal from oxidation and the use of coal for fuel.

The Industrial Revolution brought significant changes to welding techniques and equipment. In the late 1800s, fusion welding was developed, which used a carbon electrode to generate an electric arc that melted metal. This technique was used primarily for welding iron and steel, initially developed for the construction of bridges and buildings, but it soon found applications in shipbuilding, locomotive construction, and other industries. The first formal description of intentional fusion welding was published in 1881 by Auguste de Meritens, and it described a device that welded lead battery plates together using carbon electrodes. A few years later, N. Benardos and S. Olszewski, Meritens pupils, patented a machine for a welding procedure utilizing carbon electrodes and an electric power supply - the machine developed can be seen in Figure 1.1. In 1888, N. G. Slavianoff found a new technique for welding using bare metal electrodes. It is worth noting that the carbon electrodes approach was designed for structural welding, whereas the bare metal electrodes method was intended for filling holes and fixing cracks [2, 3].

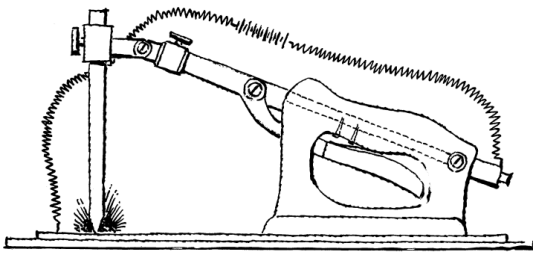

Figure 1.1: Original N. Benardos and S. Olszewski Carbon Electrode Apparatus [2].

In the XX century, welding with bare electrodes increased in popularity, mostly as a repair technique, although this method had a major problem: it produced an extremely unstable arc. To address this issue, in 1907, the Swedish inventor Kjellberg developed an electrode coating method. His work was then followed by another, in 1912, detailing the alloying and coating ingredients that may be used in flux coatings, which produce incredible welding results [2, 3].

New methods were developed over time, but metal arc welding was done manually until 1930. Some attempts at automating the process were made using continuous wire, the most effective technique was Submerged Arc Welding (SAW), in which the wire is "submerged" beneath a layer of granular fusible flux - this method is visible in Figure 1.2a [3].

Many companies experimented with the use of argon and helium as shielding gases, as welding evolved, but cost factors were against it. However, during World War II, the welding market was flooded with the demand for welding light gauge aluminium and magnesium, which were primarily used in aircraft. As a result, in October 1941, Merideth developed the first Tungsten Inert Gas (TIG) patent [4]. This new method employed a tungsten electrode, which allowed for an arc that did not melt the electrode, allowing for welds with or without filler material - Figure 1.2b shows this principle [2, 3].

Several years later, an innovative way of welding was created. In this method, the weld was shielded by inert gases, such as helium and argon, and it did not make

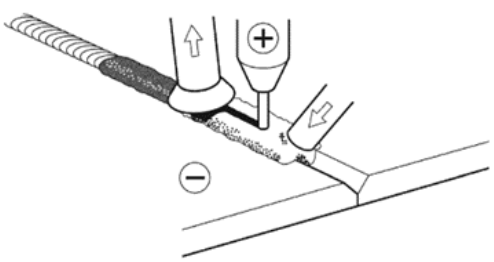

(a) Submerged Arc Welding (SAW) [3].

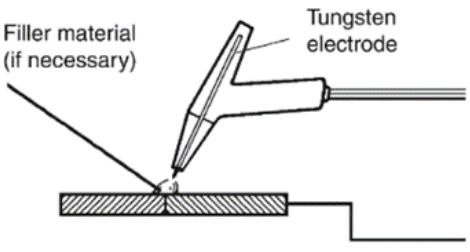

(b) Tungsten Inert Gas (TIG) [3].

Figure 1.2: Emergence of new welding techniques.

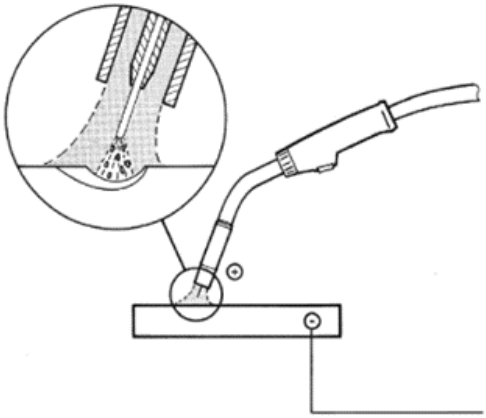

Figure 1.3: Metal Inert Gas (MIG) / Metal Active Gas (MAG) [3].

use of an electrode, instead, a metal wire was constantly fed through a spool and into the weld pool, where it melts and fuses the metal pieces together. This new technique became known as Metal Inert Gas (MIG) [3]. Because it was difficult to obtain inert gases, Lyubavskii and Novoshilov tried to employ Carbon Dioxide (CO_2) instead, despite the fact that this one caused an endless generation of spatter. They solved the issue by employing a technique known as "dip transfer". If the shielding gas used is relatively reactive, such as CO_2 or a mixture of argon and CO_2, the MIG process can alternatively be referred to as the Metal Active Gas (MAG) method [3]. This fresh strategy is portrayed in Figure 1.3. MIG/MAG welding is known for its speed and efficiency, making it popular in manufacturing and fabrication.

The development of welding machines continued, with the introduction of semi-automatic and automatic welding machines, as well as the improvement of welding equipment, by introducing welding machines that could generate high levels of electrical current to produce an arc. Additionally, gas welding equipment was developed, including oxygen and acetylene tanks, regulators, hoses, and torches. These machines and equipment increased efficiency and accuracy in welding, making it easier to join metal pieces together. The development of robotic welding machines has also been a significant advancement in welding technology. Robotic welding machines are used in automotive manufacturing, shipbuilding, and other industries where precise and repetitive welding is required [2, 3].

1.1 Problem Definition

Currently, there is a labour shortage in the welding industry [5]. Despite the fact that welding has become an essential task in the vast majority of industries, the number of technicians keeps decreasing over the years. This decline is due to a number of issues associated with this profession, including physical wear, health issues, and the difficulty and cost of learning [6]. To address these problems, the

welding industry has developed new techniques and mechanisms for training welding professionals. Along with this mission, the Institute for Systems and Computer Engineering, Technology and Science (INESC TEC) presented a proposal to create virtual reality software for new technician training. The objective of this dissertation is to explore contemporary welding training techniques and virtual reality mechanisms, with the aim of developing a system that can assist in the education of novice welders. To achieve this goal, the dissertation will investigate the challenges that exist in welding education, their sources, and potential solutions. Specifically, it will delve into the traditional welding training methods and the limitations they face, such as the high costs, safety risks, and the time and effort required to acquire hands-on experience.

Typically, welding classroom methods include lecture-based instruction, in which an instructor lectures a group of trainees on welding theory, safety procedures, equipment usage, welding techniques, and welding materials. It is also ground for demonstrations of welding techniques and safety procedures. Here, trainees group together to discuss and share their ideas, ask questions, and clarify their doubts. During classroom instruction, trainees may be present with worksheets and exercises, designed to reinforce their knowledge. Traditional classroom methods for teaching welding theory, safety procedures, and equipment use are effective, but they lack practical experience. Therefore, it is essential to supplement these methods with hands-on learning opportunities [7, 8].

The traditional hands-on learning environment for welding is a workshop or lab, where trainees can practise welding techniques on a variety of materials and receive feedback from an instructor. This hands-on approach allows trainees to develop the muscle memory and coordination required for welding and to acquire a practical understanding of the welding process. However, there are some areas where the traditional hands-on approach can be improved. First, the cost of apparatus and materials makes the training expensive, increasing the overall training price and making it difficult to practise outside of the workshop. Second, access to welding workshops can be restricted, especially in regions where there is a dearth of qualified welding instructors. Third, the traditional hands-on approach can be time-consuming and may not be suitable for pupils who require a more flexible schedule for learning. Lastly, while welding is inherently dangerous, apprentice welders are at even greater risk, given that they are still learning the proper ways to protect themselves [8, 6].

As presented by the Health and Safety Executive (HSE) [9], welding is a hazardous occupation that puts workers at risk for a wide range of health concerns, spanning from acute to chronic health problems. This activity can also have an effect on one's eyes and skin, although lung cancer is by far the most frequent of these diseases. Laid forth is a list of the most prevalent health risks associated with welding:

- **Acute respiratory health effects:**

  A short time after being exposed to welding smoke, acute symptoms manifest themselves as illnesses. According to estimates provided by HSE, between 40 and 50 welders are hospitalized every year as a direct result of breathing in metal fumes while on the job [9]. The most frequent acute respiratory disorders that are associated with welding include irritation to the throat and major airways in the lungs, acute irritant-induced asthma, metal fume fever, and acute pneumonia [9].

- **Chronic respiratory health effects:**

  After being exposed to welding fumes, chronic consequences manifest themselves more gradually and ultimately result in more severe disorders, the most common of which are lung cancer, chronic obstructive pulmonary diseases (COPD), welder's lung, and occupational asthma [9].

- **Asphyxiation when welding in a confined space:**

  Asphyxiation (suffocation from lack of oxygen), which can result in death, is a risk while welding in enclosed environments. This condition may develop as a result of prolonged contact with carbon monoxide or other shielding gases [9]. Because welding in a tight space is an operation that has a significant level of risk, it should only be done when it is absolutely essential [9].

- **Other health effects of welding:**

  Welding fumes are one of the most prominent hazards associated with the process, and they can lead to a variety of respiratory disorders. However, welding can also lead to problems with the skin and eyes, as well as neurological diseases [9].

To summarise, the main problems encountered during welding instruction are laid forth in Table 1.1. These have been divided into four categories: *economic factors*, *technical problems*, *social factors* and *training issues*.

1.2 Objectives

New approaches to teaching welding, such as Virtual Reality (VR) and Augmented Reality (AR) simulators, have numerous advantages, mainly as trainees can practise welding techniques in a virtual environment without the need for costly apparatus or materials. Besides, these simulators allow for a more immersive and adaptable learning environment, leaving room for more challenging and diverse practise scenarios. Furthermore, they allow trainees to progress at their own pace and provide a controlled environment to practise, allowing them to make mistakes and receive

Table 1.1: Main problems of welding instruction (adapted from [6]).

Economic Factors	Training comes at a high cost. The process of training demands a significant investment of time, money, and other resources. Equipment used for training needs to be maintained on a regular basis.
Technical Problems	The process of welding might result in the production of hazardous gases and contaminations. Accident-prone. Unfriendly environment. Training demands the use of specialist facilities or workshops for practise.
Social Factors	Because of the difficult conditions and the inherent dangers of the job, welding is a vocation that is stigmatized by society. The students' lack of motivation is a significant problem.
Training Issues	Complicated to learn and master. Complexity in implementing and assessing educational procedures. Self-evaluation is a component of the evaluation. Training to be a welder needs a significant amount of mentoring. On the other hand, the absence of welders generates a chain reaction that results in an inadequate supply of trained instructors. The training process takes a significant amount of time.

feedback, in a safe manner. This enables the trainees to gain a better understanding of the welding process and materials, and it enables a more individualised approach to learning, as trainees can receive individual feedback and instruction tailored to their needs [10]. On the other hand, virtual reality technology may be utilized in human-robot cooperation, in which the welder performs the weld in a virtual environment and the robot mimics the action in the real world, thus minimising the human contact with welding's inherent dangers [11].

Building upon the concepts just presented, the goal of this dissertation is to develop a virtual reality welding simulator, with a focus on creating a realistic virtual weld. In addition to the main objective, this thesis dwells on the creation of a classification system capable of identifying the simulator's key characteristics, to create a balanced simulator. Therefore, the secondary objective of this thesis is to develop a classification system for the accurate evaluation and comparison of virtual reality welding simulators.

With these objectives in mind, two set of sub-goals have been proposed. The first is for the research component of the project, and can be found in the following list:

- Examining the primary training methods;

- Identification of the most common types of arc welding;
- Identification of the most common welding positions;
- Creation of a classification system for evaluating and comparing welding simulators.

The second set of sub-goals is related with the development of a virtual reality welding simulator. This last set of sub-goals can be seen bellow:

- Creation of a virtual environment;
- Accurately capturing user movements using the HTC VIVE Pro 2;
- Implementation of welding tools, such as the welding torch, cutting pliers, and welding mask;
- Implementation of a realistic fluid model for weld simulation.

In an effort to enhance understanding of welding simulation, this dissertation endeavors to examine several crucial scientific questions.

Scientific Question 1: *How can the intricacies of welding's physical nature be accurately reproduced within the context of a virtual reality simulation?*

This inquiry forms the basis of this undertaking, as it pertains to the quest for a precise depiction of weld that reflects the physical attributes of the material in the real world.

Scientific Question 2: *In what systematic ways can virtual reality welding simulators be classified and evaluated?*

The second inquiry lays the groundwork for understanding the systematic evaluation and classification of virtual reality welding simulators, encompassing an assessment of their effectiveness, applicability, and significance.

Scientific Question 3: *In the context of welding simulators, which fundamental characteristics define an appropriate balance between cost and quality?*

The ultimate inquiry delves into the intricate interplay of attributes that a simulator must possess to be considered both cost-effective and of exceptional quality.

This scientific investigations serve as a compass for this undertaking, guiding it toward innovative insights and resolutions in the domain of welding simulation.

1.3 Expected Results

The purpose of this dissertation is to address a number of issues associated with conventional welding instruction. The utilization of a virtual reality platform is expected to lead to a more engaging and efficient training experience for welders, ultimately contributing to the enhancement of their skills, motivation, and reduction

of associated expenses. In addition, by providing a virtual introduction to welding hazards it intends to improve student safety and reduce health risks. It is also intended to address the issue of limited instructor availability by introducing personalised guidance mechanisms that can provide customised feedback to each trainee, thereby reducing wait times and allowing for more effective use of instructor time. It's anticipated that the simulator will ultimately decrease training periods while maintaining or enhancing student performance.

1.4 Work Plan

The dissertation work schedule is divided into two major sections. The first part, which involved the actual development of the virtual reality simulator, was scheduled to take place from October 3, 2022, to August 31, 2023. This part was further divided into two subtopics: "Implementation of the VR Functions" and "Fluid Simulator Development". The first subtopic took place during the month of October 2022. The second subtopic took place from November 1, 2022, to August 31, 2023.

The second part of the dissertation, which involved writing the thesis, was scheduled to take place from October 3, 2022, to September 24, 2023. This part was further divided into two subtopics: "Study of the Problem and Existing Technologies" and "Project Developed". The first subtopic took place from October 3, 2022, to March 10, 2023, with a review period scheduled for the last three weeks of March, and a submission date on March 31, 2023. The latter subtopic was scheduled to take place from April 3 to September 15, 2023, with a revision period from September 18 to September 22, 2023. The work done during this subtopic had to be submitted on September 24, 2023.

Additionally, it was planned a paper submission to the 26th International Conference on Interactive Collaborative Learning (ICL), on April 12, 2023. The paper was written between January 2, 2023, and April 4, 2023, with a revision period from April 5 to April 12, 2023. The final submission was placed on April 12, 2023. The presentation of this paper will be held between September 26, 2023 and September 29, 2023 in Madrid.

All work had to be submitted by the final planned due date of September 24, 2023. Figure 1.4 shows the timetable for this dissertation.

1.5 Organization of the Dissertation

This document is structured into five chapters. The first, and present, chapter is Introduction. The second, Theoretical Foundations, aims to provide readers with the project's context. It begins by addressing the concepts of augmented and virtual reality before proceeding to the welding subject. In the latter, the principal welding

methods and positions are presented. After the welding subject, the second chapter proceeds to present the main fluid simulators architectures, finishing with the presentation of the advantages of parallel processing. The third chapter, Virtual Reality Welding Training, reflects on the benefits and motivations of using virtual reality technology for welding training, presenting case studies and related technologies. At this level, a classification proposal is presented for the various simulators currently on the market. The fourth chapter, Virtual Reality Welding Simulator, centers on several key aspects. It delves into the creation of the virtual environment, the development of virtual welding tools, the implementation of fluid simulators for welding simulation, the rendering of the weld, and concludes by emphasizing the enhancement of the simulator through the utilization of parallel processing capabilities of graphical processing units and the methods for their effective implementation. The final chapter, Conclusion, offers an evaluation of the work accomplished throughout the project and suggests future improvements.

Figure 1.4: Gantt chart.

Chapter 2

Theoretical Foundations

This chapter is intended to provide the reader with a better background for understanding the developed project. First introduces augmented and virtual reality, highlighting their advantages and applications. Then, it explores welding, its challenges, and learning methods. Next, it covers various fluid simulator architectures. Finally, it delves into parallel processing capabilities and their benefits.

2.1 Augmented and Virtual Reality

This work uses the concept of "virtual continuum" defined by Paul Milgram and Fumio Kishino [12]. This idea refers to a continuum that stretches from the actual world, that we live in, to virtual reality, which is simulated by a computer. In the middle of these two opposites, there lies a mixed reality. This reality functions as a bridge between the two, being able to exhibit qualities that are shared by both of the other realities. As shown in Figure 2.1, augmented reality is a subcategory of mixed reality. Among the various subcategories, augmented reality is the most similar to the environment that exists in the real world. As was previously mentioned, the pole on the far right is occupied by virtual reality.

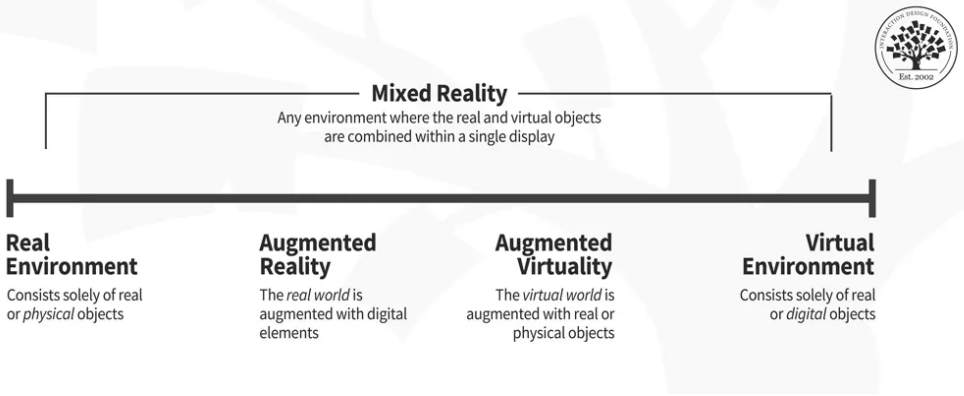

Figure 2.1: Representation of the virtual continuum [12, 13].

2.1.1 Augmented Reality

Augmented Reality (AR) is a rapidly growing technology that enhances the perception of the physical world by overlaying digital information onto real-world environments. Is based on computer vision, which allows devices to recognize and track real-world objects, and superimpose digital information onto them. Augmented Reality (AR) systems are typically composed of three main components: a display device, a tracking system, and a computing unit. The display device can be a smartphone, tablet, Head Mounted Display (HMD), or a smart-glasses. The tracking system is responsible for detecting and tracking real-world objects, and the computing unit processes the data and generates the digital information that is overlaid onto the real-world environment [14, 15].

The integration of digital information with the physical world has led to an increased interest in AR applications across various fields [6, 16, 17, 18]. In education, AR can be used to create immersive learning experiences, where trainees can interact with 3D models of complex concepts [15, 19]. In healthcare, AR can assist surgeons during complex procedures by overlaying medical images onto the patient's body. In tourism, AR can provide tourists with interactive and informative experiences by overlaying historical and cultural information onto real-world landmarks [20]. In marketing, AR can be used to create interactive and engaging advertising campaigns that allow customers to try out products virtually before making a purchase [21, 22].

Despite the numerous benefits of AR, there are still several challenges that need to be addressed. One major challenge is the limited Field of View (FOV) of current AR devices, which can hinder the user's experience [23]. Another challenge is the development of accurate tracking systems that can detect and track real-world objects in real-time [24]. Privacy concerns also need to be addressed as AR technology becomes more prevalent [25].

The future of augmented reality technology is promising, with the potential

to revolutionize the way we interact with the world. Advancements in hardware, such as the development of lighter and more comfortable HMD with wider FOV, will enhance the user experience. Improvements in computer vision and tracking systems will enable more accurate and reliable AR experiences. The integration of AR with other emerging technologies, such as artificial intelligence and 5G networks, will unlock new possibilities for AR applications [16].

2.1.2 Virtual Reality

Virtual Reality (VR) is a technology that immerses the user in a simulated environment, allowing him to interact in a seemingly real way [15]. It is typically achieved through the use of a VR headset, covering the user's eyes and ears, and, sometimes, hand-held controllers, to provide a sense of presence and physical interaction within the simulated environment. VR is designed to give users a feeling of being inside a virtual world, allowing them to explore and interact with the environment in a way that feels natural and intuitive. VR is used in a variety of applications, including gaming, entertainment and therapy [16].

This technology is increasingly being used for learning and education purposes [15]. In VR, trainees can interact with simulated environments and objects, providing a highly immersive and interactive learning experience that can engage trainees in a way that traditional methods, such as lectures or textbooks, often cannot. VR has been shown to boost trainees' motivation and engagement while also increasing their knowledge of content's spatial structure and purpose, acquisition of linguistic linkages, long-term memory retention, improved performance on physical tasks, and more [15]. On the other hand, it can be applied to technical training allowing trainees to practise complex procedures and techniques in a safe and controlled environment, before trying them in the real world. These systems are used in areas like medicine [26, 27], academics [15, 28], industry [14, 29] and even for military purposes [30, 31].

Despite the numerous advantages of VR technology, there are still a number of obstacles to overcome. The more budget-friendly VR devices, like PlayStation VR, present small FOV, leading to occlusion of user movements, and low accuracy [23]. On the other hand, the more precise ones come at a steep cost, which can limit their accessibility to a wider audience [32]. The development of accurate monitoring systems that can detect and track the user's movements and location in real-time is another obstacle. Some users may also experience motion sickness and discomfort, particularly during extended use [33].

Virtual reality technology has the potential to revolutionize how humans interact with digital content in the future. Hardware advancements, such as the creation of more lightweight and pleasant headsets with higher resolution displays, will improve the user experience. Enhancements to haptic feedback and other sensory inputs

will enhance immersion. The incorporation of virtual reality with other emerging technologies will open up new VR application possibilities [34].

Currently, there are several notable hardware solutions for VR, each of which contributes distinct features to the immersive experience. Below is a concise introduction and examination of some of the most prominent VR equipment currently available.

Oculus Rift S: The Oculus Rift S is a computer based virtual reality headgear developed by a Facebook subsidiary, the Oculus. It features a remarkable display with high resolution and a comfortable design for extended use. The Oculus Touch controllers offer accurate hand monitoring and interaction in virtual environments. Figure 2.2 demonstrates this product [35].

Figure 2.2: Oculus Rift S [35].

HTC VIVE: The HTC VIVE series, which includes the VIVE Pro and VIVE Cosmos, provides a comprehensive virtual reality experience. HTC VIVE devices are favored by both professionals and amateurs due to their room-scale navigation and precise controllers. The VIVE Pro features high-resolution displays, whereas the Cosmos' modular design provides flexibility. Figure 2.3 illustrates the VIVE Pro 2, with its hand controllers and base stations [36].

Figure 2.3: HTC VIVE Pro 2 [36].

PlayStation VR: To introduce VR to the PlayStation 4 and 5, Sony developed the PlayStation VR. With an expanding library of VR games and compatibility with PlayStation Move controllers, this equipment makes VR gaming accessible.

Opposed to the other solutions that rely on several base stations, this counts only with a single base station. Figure 2.4 presents the HMD and the base station [37].

Figure 2.4: PlayStation VR [37].

Valve Index: Developed by Valve Corporation, the Valve Index is renowned for its high-fidelity visualizations and accurate monitoring. It has finger tracking controllers for better hand presence and a wide field of view. The Valve Index is favored by VR enthusiasts in search of the best experiences. Figure 2.5 demonstrates this product [38].

Figure 2.5: Valve Index [38].

Samsung Odyssey Collection: The Samsung Odyssey series, which includes Odyssey + and Odyssey Quest, is renowned for its portability and flexibility. These Windows Mixed Reality headsets strike a balance between affordability and quality, making them a desirable option for those in search of a versatile VR solution. Figure 2.6 depicts this product [39].

HP Reverb G2: The HP Reverb G2 is distinguished by its exceptionally high resolution screens and ergonomic design. Designed in collaboration with Valve and Microsoft, this VR headset provides an immersive gaming and professional experience. Figure 2.7 illustrates this product HMD and hand controller [40].

Figure 2.6: Odyssey Quest [39].

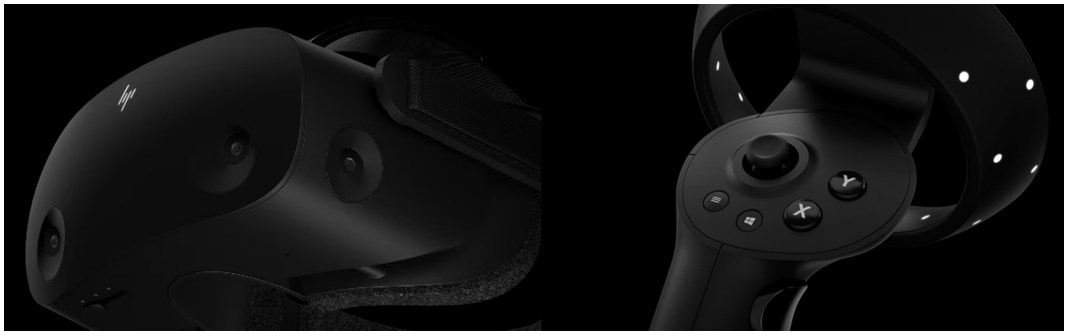

Figure 2.7: HP Reverb G2 [40].

2.2 Welding

There are many skills fundamental to the proper work of the industry. One of them is welding, a highly demanding job that poses several health risks to the worker. Even so, it is essential for the creation of many assorted products and infrastructures. This manufacturing method involves fusing two pieces together using heat or pressure, creating a junction known as a weld. The welding process is applicable to metals, thermoplastics, and wood, although the focus of this dissertation will be on metals [41]. This section will present a briefing on the two primary factors to consider when discussing welding: type and position of welding.

2.2.1 Welding Types

As mentioned before, welding has been in use for several years, and because of that, it has a broad range of uses, shaping itself to each one of them, leading to the development of numerous welding processes [3]. There are two classifications for these: pressure welding and fusion welding. In the first category are resistance welding, friction welding, ultrasonic welding, and other techniques. The second category includes gas welding, arc welding and power beam processes. Figure 2.8 presents a graph with these procedures.

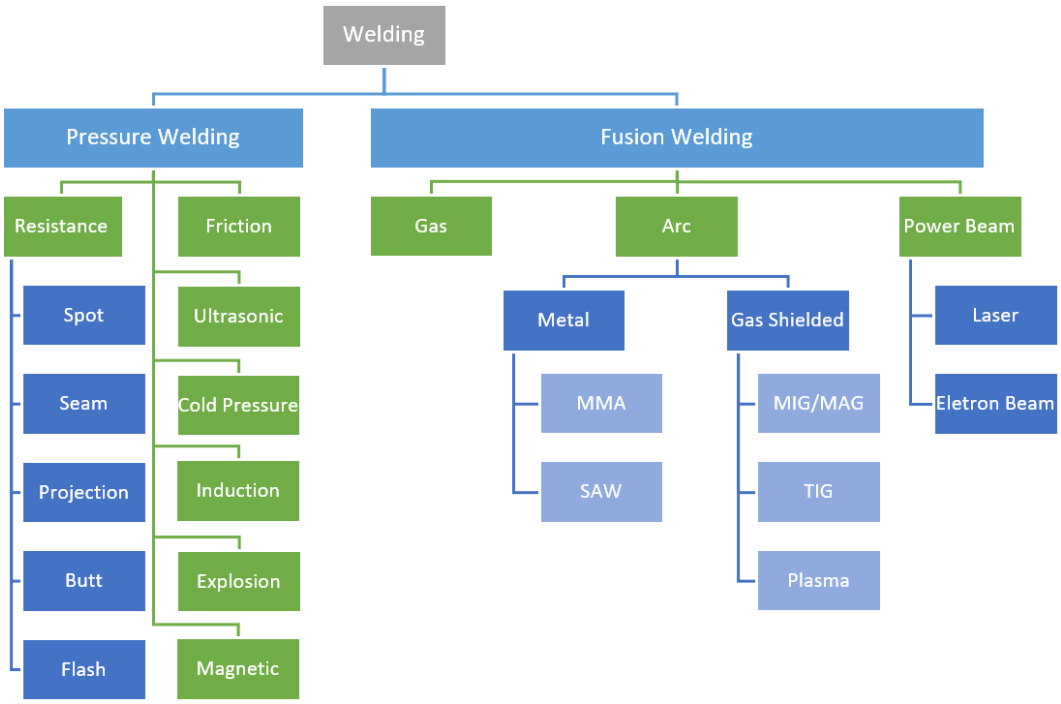

Figure 2.8: Most common welding methods (adapted from [3]).

This dissertation will focus on arc welding methods. According to the American Welding Society (AWS) [42], arc welding is a welding technique that employs an electric arc to melt and connect metals. An electric charge is transmitted through an electrode in this procedure, creating an arc between the electrode and the object. The arc's heat melts the base metals and forms a weld pool, which cools and solidifies to form a permanent joint. Shielded Metal Arc Welding, Gas Tungsten Arc Welding and Gas Metal Arc Welding are a few examples of arc welding techniques. Each method employs a distinct type of electrode or filling substance and may necessitate the use of a distinct type of shielding gas. Arc welding is used in many sectors, including production, building, and repair. It is a flexible and cost-effective welding technique that can be used to connect a broad range of metals and alloys.

Shielded Metal Arc Welding

Shielded Metal Arc Welding (SMAW), also known as Stick Welding, is widely regarded as the industry's most popular welding technique. It is highly adaptable and requires minimal apparatus, making it suitable for use in confined spaces or at a considerable distance from the welding power source, and when there is rust, oil, and other contaminants at the weld joint [43, 44]. It is an arc welding technique in which an arc is formed between a covered electrode and the weld pool. The weld is formed using the electrode's metal, as the filling substance, and the flux covering, to

produce the shielding gas. This method of welding does not require the application of force [45].

A SMAW machine comprises a power supply and two wires. One provides power to the weld via the torch, and the other completes the circuit by acting as a ground terminal. The electrode, inserted into the torch, can be made of various materials and has multiple diameters. It consists of a metal rod covered with a dense coating of flux, which ignites in the arc to produce a shielding gas for the weld pool. As the metal cools, the flux hardens into a thin, brittle coating known as slag, which must be broken and scraped away [44]. Figure 2.9a shows a diagram for this process and Figure 2.9b shows the real weld technique.

Stick welding can yield excellent results, but it normally requires the expertise of a professional welder to achieve them, even though it has a low learning curve. Typically, negligible heat input produces a thin microstructure in the welded metal. This results in outstanding mechanical properties. However, slag inclusions may occur if the slag that protects the molten weld metal from the atmosphere is not correctly cleaned between passes and at the beginning and conclusion of each weld. Multiple beginnings and pauses in large welds frequently lead to defects [43].

Despite the relatively low cost of the equipment, the overall cost of employing this method can be substantial due to the low deposition rate, or the quantity of weld metal deposited per hour. Given that the average length of a consumable electrode is only 35 centimetres, the discharge must be interrupted frequently to replace the electrode. This results in downtime, fragment loss, and overall inefficiency, all of which increase expenses [43]. Table 2.1 provides the principal advantages and limitations of SMAW.

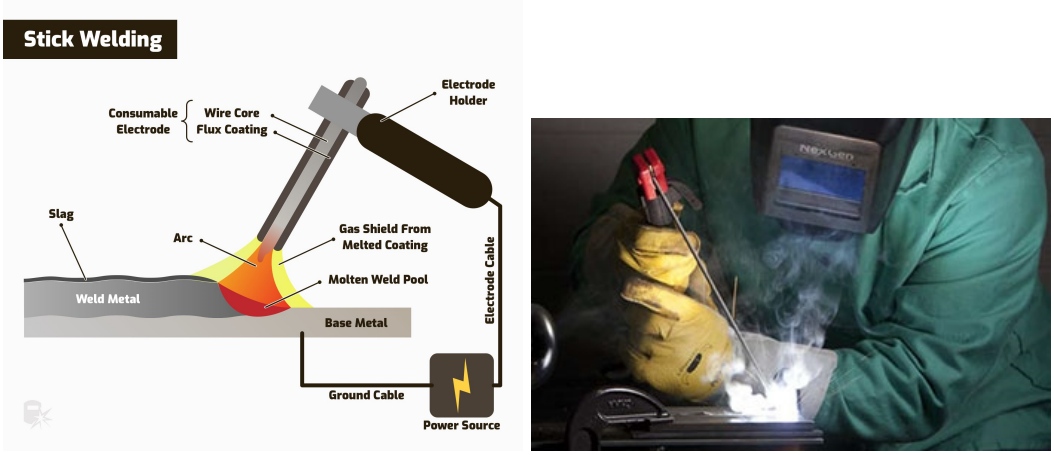

(a) Stick welding diagram [44]. (b) Stick welding [43].

Figure 2.9: Shielded Metal Arc Welding, also known as Stick Welding, is widely regarded as the most popular welding technique [43].

Table 2.1: Advantages and limitations of SMAW (adapted from [44]).

Advantages	Limitations
Low learning curve	Thin metal can be hard to work
Affordable equipment	Generates a lot of heat
Not contaminant sensitive	Takes a lot of time
Can weld almost any metal	Generates slag

Tungsten Inert Gas

Gas Tungsten Arc Welding (GTAW), also known as TIG, is frequently regarded as the most expensive and high-quality form of arc welding [43, 44]. The primary distinction between TIG and other processes lies in the electrode in the torch: it is a short and sharpened tungsten shaft, not wasted in the process. Instead, the operator inserts a long rod of filler metal into the weld pool while operating the torch with the other hand. Similar to a flame torch, the electrode only strikes and maintains the arc that melts the metal. The operator's ability to control the torch, regulate the temperature, and feed the filler rod at the optimal rate is crucial to achieving successful results. To shield the weld, the TIG torch transports pressurised inert gas to saturate the arc region [44, 46].

Although there are some automated applications, it is typically performed manually. A professional welder can deposit approximately 0.25 kilogrammes of weld metal per hour at a travel rate of approximately 2.5 to 7.5 centimetres per minute. Because the travel speed is relatively slow, the heat input per centimetre of weld can be relatively high, resulting in outstanding weld metal fusion. This can lead to distortion in narrow sections [43].

The heat input per deposited weld metal is low because manual TIG welding operates with a relatively low current and voltage and cool filler metal is introduced to the puddle. This produces a much finer particle size and superior mechanical properties compared to other methods. There are no micro-inclusions to reduce mechanical properties because there is no flux. On carbon and stainless steels, pure argon is typically used as the shielding gas, resulting in very low oxygen content in the weld metal and exceptional mechanical properties [43, 44]. Figure 2.10a shows a diagram for this process and Figure 2.10b shows the real weld technique. Table 2.2 provides the principal advantages and limitations of TIG welding.

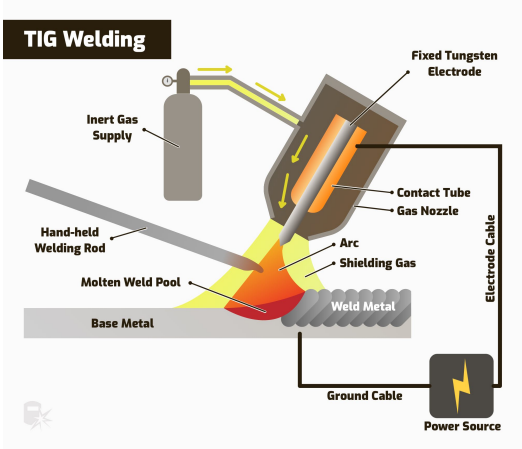

(a) TIG welding diagram [44].

(b) TIG welding [47].

Figure 2.10: Gas Tungsten Arc Welding, also known as Tungsten Inert Gas, is frequently regarded as the most expensive and high-quality form of arc welding [43, 44].

Table 2.2: Advantages and limitations of TIG (adapted from [44]).

Advantages	Limitations
AC TIG welds aluminium and magnesium alloys	It takes more skill and experience to master
DC TIG welds brass, copper, steel, stainless steel, and titanium	TIG machines are more costly
Best quality, highest precision	
Able to weld very thin materials	
No slag	

Metal Inert Gas / Metal Active Gas

Gas Metal Arc Welding (GMAW), also known as MIG welding, is a welding process that uses a continuous solid wire electrode and an inert shielding gas to protect the weld pool. If, instead of inert gas, it is applied an active gas this process is called MAG welding. The electrode is fed through a welding gun and melted by an electric arc, which creates the weld pool that fuses the two base materials together [44, 48, 49]. Figure 2.11a shows a diagram for this process and Figure 2.11b shows the real weld technique.

There are four main types of GMAW: short-circuiting, globular, spray and pulsed [43, 44, 51]. In short-circuiting transfer, the welding current is pulsed on and off at a high frequency, causing the electrode to repeatedly touch the base material and create small droplets of molten metal that are transferred to the weld pool. This type of transfer is commonly used for welding thin materials and produces a smooth and low-penetration weld. In the globular transfer, high current

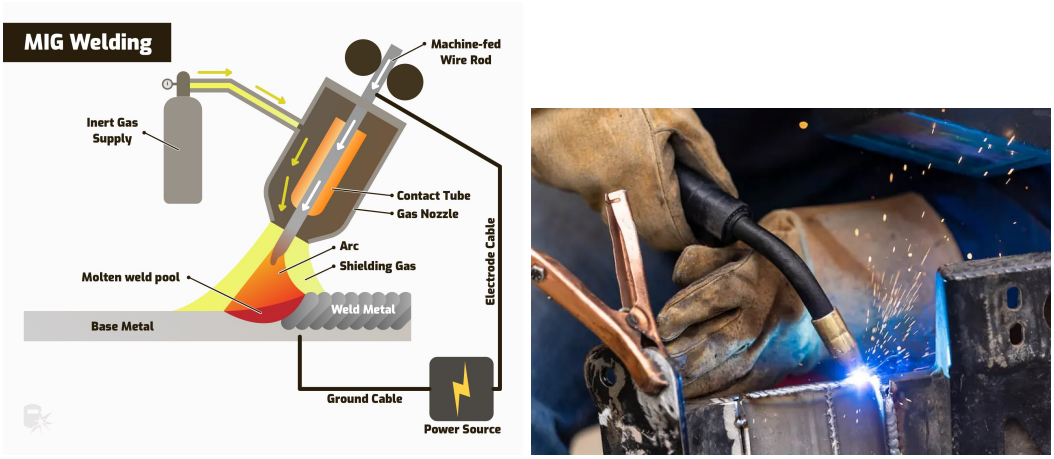

(a) MIG/MAG welding diagram [44]. (b) MIG/MAG welding [50].

Figure 2.11: Gas Metal Arc Welding is a welding process that uses a continuous solid wire electrode and an inert (MIG) or an active (MAG) shielding gas to protect the weld pool [44, 48].

and voltage are applied, resulting in an uncontrolled short-circuit. This produces a droplet of molten metal that falls into the weld pool and typically has a larger diameter than the wire supplied. This technique allows for thicker material welding and greater penetration, but it produces a large deal of spatter, limiting its application to flat and horizontal welds. Moreover, lack of fusion in the weld is quite common, and the high heat input causes changes in the microstructure of the metal, thereby degrading the weld quality. Spray transfer, on the other hand, uses a higher welding current and voltage to create a spray of fine molten droplets that are transferred to the weld pool. This form of transfer, much like globular, is used for thicker materials and produces a deeper penetration weld, but it can still produce strong, aesthetically pleasing welds with minimal spatter because no short circuits occur. The pulsed mode is typically used for welding stainless aluminium and steel. It incorporates the benefits of other transfer methods while reducing their limitations. The substance is conveyed in the form of controlled droplets. The method's reduced thermal input enables it to be used on thinner materials, furthermore, the pulses produce spatter-free welds.

The GMAW process is commonly used in the automotive, construction, and manufacturing industries due to its versatility and relatively high welding speed. It is capable of welding a wide range of materials, including mild steel, stainless steel, and aluminium, and can be used to produce both thin and thick welds, with low levels of distortion. It is commonly used in industries such as automotive, aerospace, and construction [49]. Table 2.3 provides the main advantages and limitations of MIG/MAG welding.

This method is suitable for both manual and automated welding applications. In manual GMAW, the welder controls the welding gun and manually feeds the

Table 2.3: Advantages and limitations of MIG/MAG (adapted from [44]).

Advantages	Limitations
Good for production welding	Wind can blow away the shielding gas
Continuous wire feed	All paint and rust must be removed
Good heat control	
Clean welds	

wire into the weld pool. In automated GMAW, the welding gun is mounted on a robotic arm or another automated system, and the wire is fed automatically into the weld pool [42]. The AWS has established numerous standards and guidelines for GMAW, including AWS D1.1/D1.1M:2020 Structural Welding Code - Steel [52], which provides requirements for welding steel structures using GMAW and other welding processes.

2.2.2 Welding Positions

Welding is necessary for a variety of applications, therefore, personnel must be trained to be adaptable. In order to accomplish this, a number of "welding positions" have been developed, which, according to the International Organization for Standardization (ISO) 6947 [53] and American National Standards Institute (ANSI)/AWS A2.4 [54], can be classified into two groups (planes and pipes) and further subdivided based on orientation, location relative to the welder, and movement [6, 55, 56]. There are four primary positions in the first category: flat (1), horizontal (2), vertical (3), and overhead (4). The second group consists of autorolled (1), horizontal fixed (2), vertical fixed (5), and inclined rolled (6). In addition to plate or pipe, a position type can also be defined as fillet weld (F) or groove weld (G). By integrating these classification techniques, it is possible to differentiate between all welding positions, Figure 2.12 illustrates the most common ones. Each welding position requires the welder to adopt a specific body position, hand position, and torch angle. The welder must also be aware of the different welding techniques and the type of welding equipment that is required for each position.

2.3 Fluid Simulators

Fluids are present in all areas of the universe, exhibiting a wide range of shapes and exerting influence on several aspects. The dynamics of fluids play a fundamental role in shaping the environment and are integral to a wide range of natural processes, spanning from the huge oceans that surround continents to the intricate dewdrops

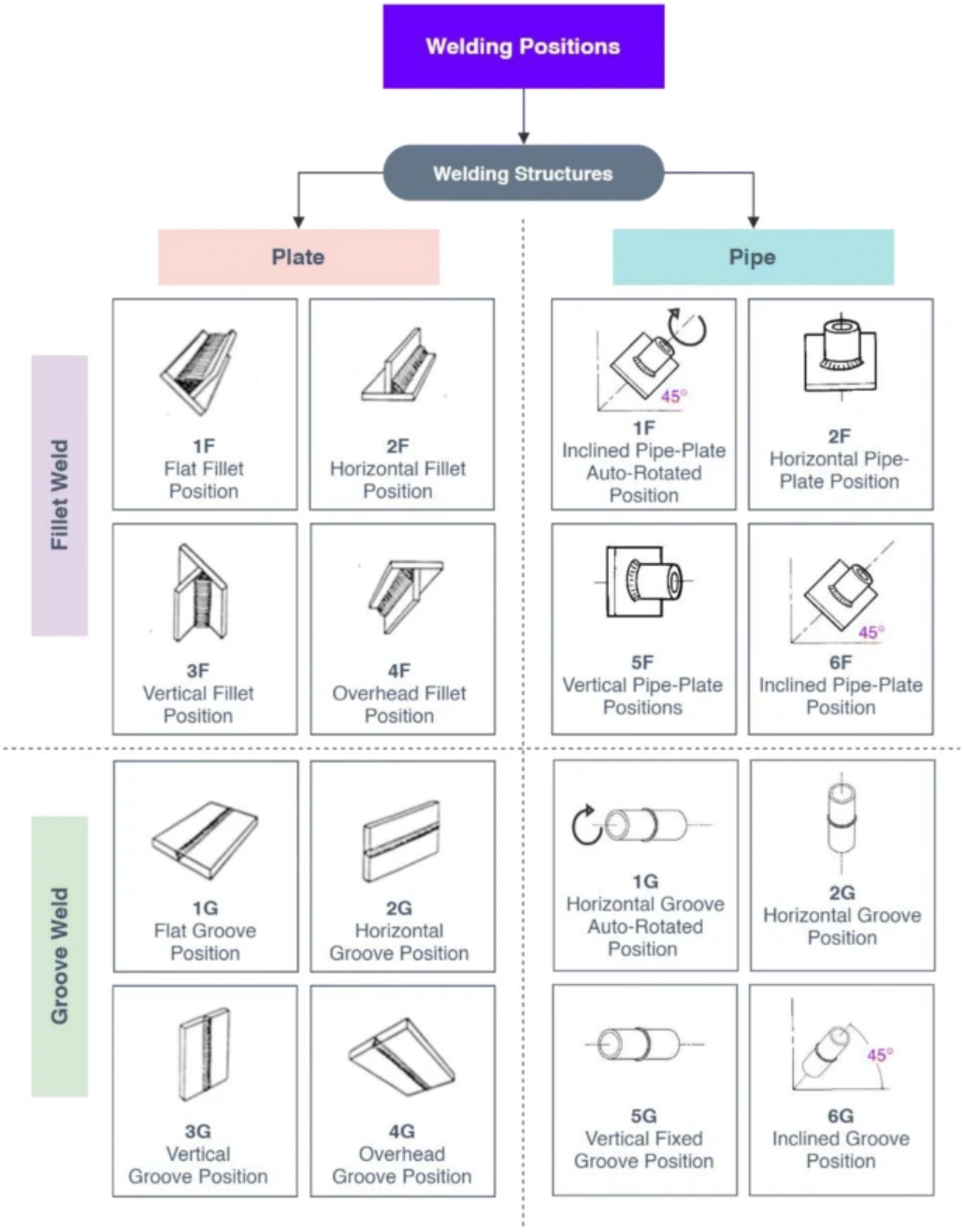

Figure 2.12: Most common welding positions [6].

found on leaves in the morning. The omnipresence of fluid behavior and its numerous applications across scientific, industrial, and creative areas highlights the importance of understanding this phenomenon [57].

The central focus of this thesis pertains to the application of virtual reality in the context of welder training, which exhibits an intriguing correlation with the domain of fluid dynamics. The convergence of these seemingly diverse realms is attributed to their similar dynamics of transition. The molten weld displays fluid-like properties. The motion and solidification of the object demonstrate similarities to the fluidic properties observed in dynamic simulations. Just as rivers shape their paths through terrains, molten metal flows along seams and joints, adhering to principles akin to those governing fluid dynamics. The comparison stated above serves to clarify the extensive knowledge that fluid simulators offer in the realm of studying and improving welding simulators.

Moving fluidly to subsequent topics, it will now be explore the complex structures that form the foundations of fluid simulators. There are three main architectural structures that serve as the foundational framework of fluid dynamics, these are Smoothed-Particle Hydrodynamics (SPH), Lattice Boltzmann Method (LBM) and Computational Fluid Dynamics (CFD). In addition to these, hybrid architectures are also prevalent, amalgamating various aspects from each methodology to tailor them optimally for the desired application.

2.3.1 Smoothed-Particle Hydrodynamics (SPH)

The Smoothed-Particle Hydrodynamics (SPH) architecture stands out as a distinctive and innovative methodology within the domain of fluid dynamics simulation. This approach, considers the fluid as an assemblage of discrete particles, each gifted with attributes such as mass, position, and velocity. With this technique, the SPH method can avoid traditional grid-based methods [58].

SPH's operations are characterized by its focus on local dynamics, wherein computations are conducted in proximity to nearby particles within a specified radius. This localized approach ensures that interactions and influences are confined to a designated region, harmonizing the evolution of fluid behaviors [58].

The merits of SPH are evident in its agility in accommodating irregular geometries and intricate boundaries, making it well-suited for scenarios replete with fluid free surfaces, splashes, and fluid-structure interactions. Furthermore, SPH inherently captures fluid-structure interactions, rendering it a choice methodology for simulations involving immersed objects or deformable materials [58].

However, the particle-based nature of SPH demands substantial computational

resources due to the intricate interactions between particles and the intricate neighborhood calculations intrinsic to the approach. Accurate representation of boundaries can also pose challenges, necessitating specialized techniques to mitigate artifacts caused by them [58].

SPH's applications span diverse domains, from astrophysical investigations on galaxy formations and stellar collisions, to fluid animation in visual media that brings water simulations and splashes to life. It finds utility in oceanography by dissecting ocean currents and wave interactions, while also delving into biomechanics to model blood flow and physiological fluid phenomena [59].

In conclusion, the Smoothed-Particle Hydrodynamics (SPH) architecture is an innovative and flexible method for simulating fluids, offering a novel perspective by treating fluid as a collection of particles. Its applications span numerous scientific and artistic fields, enhancing the comprehension of fluid phenomena and their depiction in a variety of contexts.

2.3.2 Lattice Boltzmann Method (LBM)

The Lattice Boltzmann Method (LBM) stands as a numerical technique deployed to simulate fluid dynamics with a foundation grounded in statistical mechanics. Operating within a discretized space known as a "lattice", the LBM diverges from the conventional simulation approach of directly tackling differential equations governing fluid dynamics. Instead, it engages discrete probability distributions as a fundamental framework [60].

At its core, LBM involves the division of each lattice cell into a multitude of conceivable "directions". Each direction corresponds to a specific probability distribution that encapsulates the likelihood of a particle moving in that particular direction. Through successive time steps, particles within cells undergo interactions and recalibrate their respective probability distributions. This intricate process effectively replicates the nuanced dynamics of fluid particles, akin to particle interactions and movement. This process is illustrated in Figure 2.13 [60].

A distinctive attribute of LBM resides in its capacity to converge, over time, to macroscopic equations, notably exemplified by the Navier-Stokes equations. This convergence endows the method with the ability to infer macroscopic fluid properties from microscopic simulations, presenting a bridge between these diverse scales of analysis [60].

The LBM framework offers distinct advantages. In particular, it excels at capturing complex fluid phenomena, encompassing multiphase flows and intricate fluid-particle interactions. Additionally, the discrete nature of the approach makes it great for parallelization. Furthermore, LBM exhibits inherent adaptability to irregular geometries and intricate boundaries, enabling realistic simulations in diverse real-world scenarios [60].

However, it is essential to acknowledge certain limitations. The implementation of LBM demands a comprehensive understanding of probability distributions, collision mechanics, and propagation dynamics, rendering it complex and potentially challenging. Moreover, in scenarios where precise numerical accuracy is of special importance, LBM may not outperform traditional methods [60].

LBM's applications extend across diverse domains. In the realm of biology, it facilitates the modelling of biological fluid dynamics, shedding light on phenomena such as blood flow patterns and cellular behaviors. Within engineering, LBM navigates complex flows around intricate geometries, offering insights into aerodynamics and hydrodynamics. In geophysics, it unveils the intricacies of fluid movement within subterranean reservoirs. Additionally, LBM proves valuable in investigating multiphase scenarios, encompassing fluid-particle interactions, bubble dynamics, and the characteristics of foams [60].

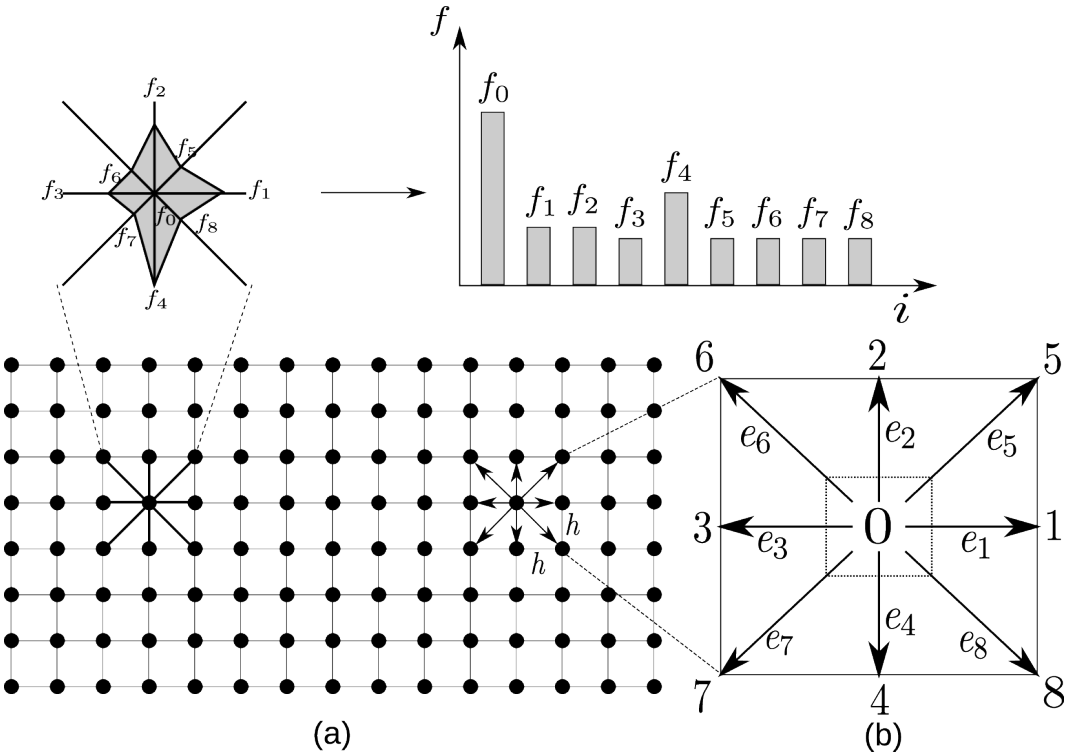

Figure 2.13: Probability distribution of a cell in the LBM architecture [60]

2.3.3 Computational Fluid Dynamics (CFD)

Within the realm of fluid dynamics simulation, Computational Fluid Dynamics (CFD) mesh based discretization emerges as a cornerstone methodology. This approach involves the division of the fluid domain into a structured or unstructured grid, referred to as a "mesh". Diverging from certain other techniques that employ

discrete particle models, CFD undertakes the direct resolution of governing partial differential equations to describe the fluid behavior [61].

At its core, CFD's fundamental principle resides in the discretization of the fluid domain into discrete cells, constituting the mesh's building blocks. These cells serve as computational entities where fluid attributes are evaluated, and equations are systematically solved. Of paramount significance, the Navier-Stokes equations, encapsulating the conservation of mass, momentum, and energy within a fluid, serving as a backbone for the CFD. These equations are discretized across the mesh to yield an approximation of the fluid's continuous behavior [61].

A pivotal aspect of CFD lies in the meticulous establishment of boundary conditions, which prescribe how the fluid interacts with the domain's boundaries. These conditions are instrumental in facilitating simulations that mirror real-world scenarios, ensuring the precision and relevance of the results [61].

CFD offers distinctive advantages. Its inherent versatility empowers it to address an expansive spectrum of fluid scenarios that encompass both incompressible and compressible flows, laminar and turbulent flows, as well as intricate multiphase and heat transfer phenomena. By directly engaging with the resolution of the governing equations, CFD ensures a heightened level of fidelity in capturing intricate fluid behaviors, rendering it a potent tool for engineering and scientific analyses. However, there are disadvantages that must be considered. The quality and resolution of the mesh substantially influence the accuracy of simulations. An inadequately designed mesh can yield erroneous outcomes or numerical instability. Additionally, the computational resources required for high-fidelity simulations can be substantial due to the computational complexity engendered by solving governing equations on a discrete mesh [61].

The CFD architecture finds extensive utility in aerospace and automotive engineering, helping to optimizing vehicle geometries. Furthermore, environmental studies utilise CFD to simulate atmospheric and oceanic flows, enabling insights into climate dynamics and in the dispersion of pollutantss. In the realm of chemical and process engineering, CFD aids in refining reactors design, forecasting mixing patterns, and analysing heat and mass transfer mechanisms [61].

In summation, Computational Fluid Dynamics (CFD) assumes a pivotal role in the exploration of fluid behaviors through numerical simulations. Operating by directly addressing governing equations within discretized grids, CFD empowers comprehensive insights into fluid dynamics across diverse realms. Its versatile applicability underscores its relevance in both industrial and scientific contexts, enriching the understanding of fluids.

2.4 Parallel Processing

Parallel processing arises as a cornerstone strategy in the landscape of contemporary computational science, transforming how researchers approach complex simulations and computations. At its core, parallel processing exemplifies the concept of simultaneous execution by orchestrating the concurrent implementation of multiple computational tasks. This method, which utilizes the combined computing capacity of a large number of processing units, has not only revolutionized scientific progress, but has also vast applications in a variety of fields. Parallel processing appears as a transformative force, specifically in the context of fluid simulation [62].

Parallel processing relies on concurrency to accelerate computation, by decomposing intricate issues into smaller segments, that are then processed simultaneously by distinct computing units. This coordinated effort reduces the overall processing time, bringing in quicker results that would be difficult under sequential processing [62].

In operation, parallel processing distributes tasks across multiple processing units, an idea that is particularly applicable to Graphics Processing Unit (GPU) and multi-core Central Processing Unit (CPU). In the field of fluid simulation, this method coordinates the concurrent computation of sophisticated fluid dynamics across multiple fluid domain segments. In contrast to sequential execution on a CPU, in which tasks unfold one after the other, parallel processing utilizes the combined power of GPU and multi-core CPU to simultaneously process distinct simulation segments [62].

There are numerous advantages of parallel processing over the conventional sequential processing. First, it increases efficiency by simultaneously completing multiple tasks, thereby drastically reducing simulation time. Second, parallel processing effectively manages the computational complexity inherent in intricate simulations by dividing the burden into manageable portions that are executed concurrently. In addition, the specialized architecture of a GPU, which is optimized for parallel computations, exponentially increases computational capacity in comparison to a standard CPU [62].

Parallel processing is particularly significant in the context of fluid simulation. Simulation of fluid dynamics use a large number of complex computations for each particle. Parallel processing's concurrent execution increases simulation performance exponentially. This accuracy not only results in faster outcomes, but also fosters enhanced precision and realism, which are essential characteristics for analyzing complex fluid behaviors. Parallel processing is unquestionably advantageous for this endeavor and establishes an indispensable link with fluid simulation, accelerating the procedure while enhancing its realism.

2.5 Conclusion

With the advancement of technology, there has been a rise in the creation and use of augmented and virtual reality applications. In this manner, these have proven to be excellent tools in the various sectors where they are incorporated, from applications for learning and education, to military and industrial settings, or even for the purposes of entertainment.

As presented in Chapter 1, welding, despite being a hazardous and demanding task, is essential to the industry's operation. It has been utilized since the Bronze Age and has evolved into what it is today. Even though it is a profession with a long history and is fundamental to the market, there is a developing shortage of qualified professionals. This deficiency is primarily due to issues with health, education, and the associated costs. As a result, there has been a demand for the adoption of VR and AR technologies in an effort to mitigate these issues.

As previously stated, there are numerous varieties of welding, with electric arc welding being the most common [42]. There are three categories within this one: SMAW, TIG, and MIG/MAG. It is also worth noticing that, in order to facilitate the learning process, associations have developed standards to classify the numerous welding positions.

In the realm of fluid dynamics, the pursuit of accurate and versatile simulations has spurred the development of diverse architectures, each with its unique attributes and applications. This chapter embarked on an exploration of three prominent fluid simulation methodologies: the Smoothed-Particle Hydrodynamics (SPH), Lattice Boltzmann Method (LBM), and the Computational Fluid Dynamics (CFD) architecture. Each methodology, driven by its underlying principles and computational mechanisms, brings forth a distinct lens through which fluid behaviors can be understood and predicted. Moreover, the realm of fluid simulation has witnessed the emergence of hybrid approaches, wherein the fusion of methodologies enriches simulation capabilities. The synergistic union of LBM and SPH, for instance, opens avenues to simulate complex multiphase flows with enhanced accuracy, merging the advantages of both particle-based and lattice-based paradigms.

Parallel processing is becoming a crucial tool in the world of computing, as it offers the potential for significant increases in speed and efficiency across a broad range of applications. In the context of this thesis, and specifically in fluid simulators, the ability to distribute the processing of the equations that characterise the fluid over multiple units makes it possible to obtain faster, more accurate and more realistic results, making it a crucial instrument for this endeavour.

Chapter 3

Virtual Reality for Weld Training

This chapter is meant to give the reader an overview of the VR welding simulators for training current state. It starts by presenting the motivation behind these solutions, then goes over a classification proposal for these simulators, followed by related works that study the efficiency and impact of VR weld training, and ends by presenting some commercial solutions.

3.1 Motivation

Welding is a critical skill in the majority of sectors, as previously stated. As a result, constant efforts have been made to identify the most efficient and cost-effective techniques for teaching new welders [63]. Welding training programs have been around for almost as long as welding has been in use. The evolution of these training technologies may be traced back to simple mechanical welder trainers, and continues through increasingly complicated mechanical systems, and finally to computer-based teaching systems [63].

As part of their training and education, students who are learning the fundamentals of welding through hands-on experience utilize a significant amount of expensive welding materials. In addition, the welding industry is continuously searching for more trained welders, for this reason, schools need to continuously be looking for new ways to get students ready for the field as quickly as possible. On the other hand,

learning this method is challenging both for the apprentice and the trainer. Furthermore, gloves, a helmet, and other protective items make it difficult for students to move and see well, hindering their education and diminishing their confidence. Furthermore, the trainee is continuously troubled by the heat as well as the sparkling and loud noise, which causes him to worry that he may be harmed [64].

Expert welders understand how to decode information from the welding pool, which allows them to perform high-quality welding. Meanwhile, the trainees have no idea what they should be doing or how they should adjust their behaviour based on the visual cues they are given.

The difficulty in effectively passing on knowledge from trainer to apprentice is one of the primary challenges that must be overcome throughout the training of welders. The transmission of theoretical information is done through lectures, whereas the transmission of practical knowledge is done through demonstrations. However, passing on information through demonstrations is difficult due to the fact that the apprentice is unable to follow the body movement of the trainer when they are welding at the same time. This is because of the constraints imposed by the gear welders are compelled to utilize in their work. To be able to look directly at the weld, which is essential for the apprentice to understand the construction of the weld pool, it is necessary to wear a welding helmet. However, this drastically reduces the trainee's FOV and luminosity, which results in only the brightest areas, the welding area, being visible.

The simulator's primary function is to offer the trainee directional cues in the form of visual, tactile, and/or audible feedback. The trainee may be able to obtain advice in real time on how to modify his position and the way that he welds [63, 64], for example, by providing visual guides to help him follow the correct path while welding. They illustrate different indicators such as the torch's trajectory, travel angle, work angle, and Contact to Work Distance (CTWD). These indicators change colour and shape depending on the position and movement of the user. Fig. 3.1 illustrates how some simulators implement the visual feedback system [65].

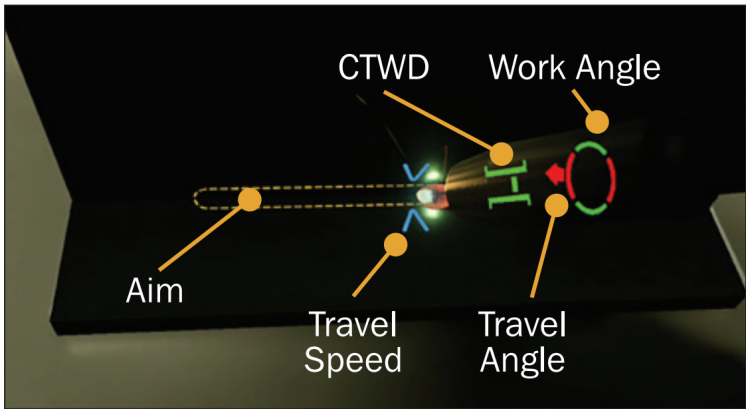

Figure 3.1: Example of VR visual feedback system [65].

Nonetheless, the VR system also makes it feasible to shorten the amount of time spent training since trainees may weld at the same time that they are getting knowledge. This is not possible in traditional training methods, where the trainees are limited to observing the instructor's demonstration without being able to practise themselves.

Finally, the goal is to give trainees their first taste of welding in a virtual environment. This way, schools can save money on supplies, while still preparing trainees for the rigours of welding, including the loudness, sparks, and fumes to which they will be exposed.

3.2 Related Works

As technologies improve, a number of researchers examine the created applications in an effort to continue their development. Virtual reality-assisted welding is not an exception. Chan *et al.* [6] conducted a comprehensive analysis based on papers published between 2000 and 2021 to determine the primary functionalities that a VR simulator for welding should have, as well as the most common types of exercises and welding processes. According to the research conducted, a welding simulator should contain three primary categories: *Welding Training*, *Post-Training Assessment* and *Instructors' Assistance*.

- The first is the use of the simulator for welding instruction, which includes the entire virtual world and the simulator's feedback mechanisms used to instruct the welder. Figure 3.2 illustrates the primary feedback methods utilized by simulators.

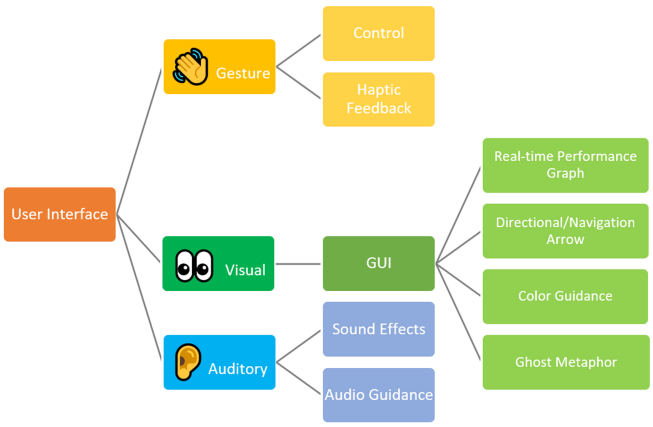

Figure 3.2: Primary feedback methods utilized by welding simulators (adapted from [6]).

- The second focuses on the system's ability to collect and retain welding data in order to analyze and enhance the student's performance at a later stage.

- The third concentrates on teacher-specific features that allow monitoring the learner during, or after, the practical session. There are also cases of systems that allow the instructor to interact with the learner in real-time in order to better assist him.

As mentioned in Subsection 2.2.2, a trainee must learn several welding positions. According to a study conducted by Chan *et al.* [6], depicted in Figure 3.3, the majority of studies carried out focus on plate positions, specifically, on 1F and 1G. However, while these positions are encountered regularly by welders, newer simulators should aim to include as many other positions as possible. The study shows that there are almost no references to pipe positions, indicating a need for correction in newer simulators.

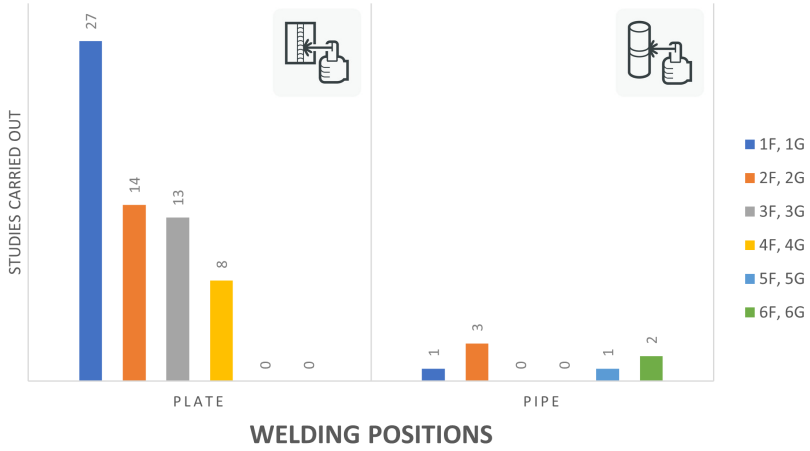

Figure 3.3: Welding positions according to the number of studies carried out (adapted from [6]).

Based on the findings of Chan *et al.* [6] study, one can draw the conclusion that the majority of the currently available welding simulators concentrate on the processes of Gas Metal Arc Welding (GMAW). It would be useful if the future developed welding simulators incorporated additional welding procedures so that welders may be better prepared by using them. A graph was generated by these researchers and is displayed in Figure. 3.4, which shows the number of papers published on these topics, that were categorized according to the type of welding performed.

In addition to studies conducted to improve welding simulators, there are also studies conducted to verify their effectiveness. Stone *et al.* [63] compare the cognitive and physical effects of simulators and traditional training. In order to do this, two classes were developed, one with a 100% traditional training component (TW) and the other with a 50% virtual training component (VR50), both of which were subjected to two weeks of instruction in order to gain certificates for four welding

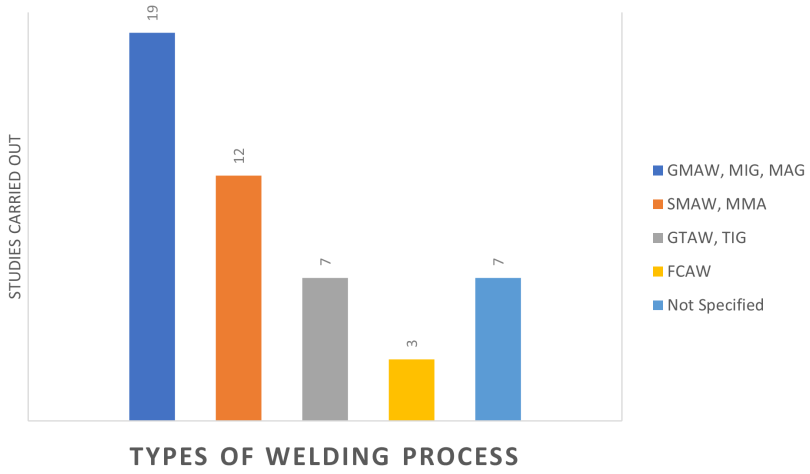

Figure 3.4: Welding processes according to the number of studies carried out (adapted from [6]).

positions. During training, students were required to use electromyograph (EMG) electrodes to analyze muscle activity accurately.

This study found that the use of a VR simulator in welding training allowed training students with the same, or more, efficiency as the traditional method, the results being present in Figure 3.5.

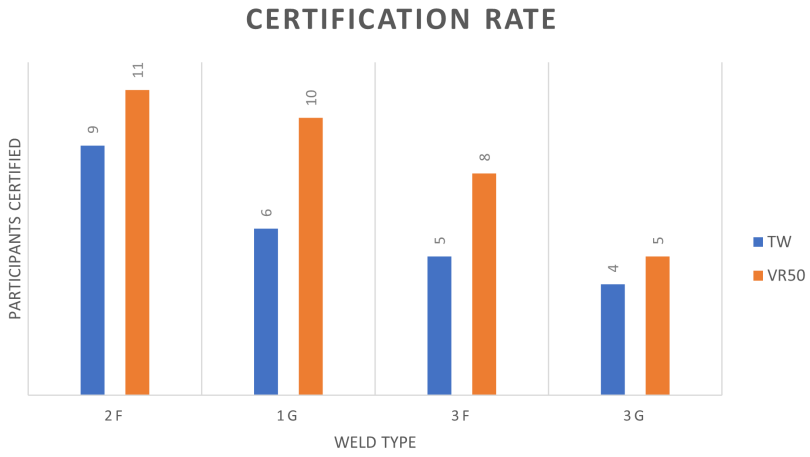

Figure 3.5: Certification rate for each class. Even though there was no significant difference in the certificates obtained, the VR50 class earned more certifications and in position 1G the difference was practically substantial, proving that the VR system performed slightly better (adapted from [63]).

Moreover, by providing frequent feedback, the trainees didn't need to spend time asking the instructor for assistance, leading to an effective decrease in training time by 18% to 20%, visible in Figure 3.6. While there were no significant differences in physical or cognitive development between the VR and traditional training groups for

most positions, the VR group showed greater muscle activity and utilized alternative welding techniques for position 1G (Flat Groove Position), demonstrating that the use of VR technology motivates the trainees to discover new methods, different from the ones being taught. Additionally, there were no differences in mental load between the two groups. Overall, the study suggests that the use of VR simulators in welding training can be a beneficial tool for students and instructors.

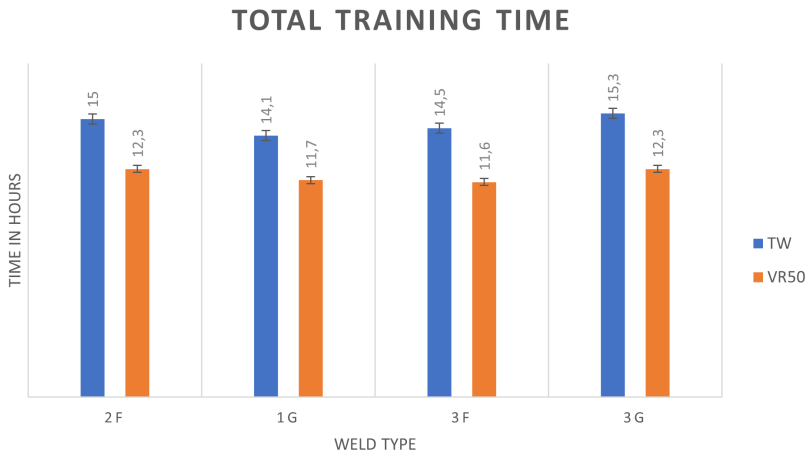

Figure 3.6: Total training time per group. As seen by the graph, the VR system allowed for a considerable decrease in training hours when compared to the traditional approach (adapted from [63]).

3.3 Commercial Solutions

In this section, three virtual reality welding simulators will be presented: the Mobile VR Welding Kit, CS WAVE, and ARC+. This selection encompasses a range of options, including both more affordable and less sophisticated simulators, as well as higher-end, advanced solutions. The choice of these simulators is based on their market presence and their ability to showcase the diverse landscape of VR welding technology.

3.3.1 Mobile VR Welding Kit

In 2021, Isham *et al.* [66] proposed a low-cost mobile welding VR simulator, the Mobile VR Welding Kit. This simulator utilizes a 3D printed torch, a set of markers, and two smartphones, one for tracking the markers and the other for the head-mounted display. Despite its functionality and cost-effectiveness, this solution has certain limitations. For instance, the narrow FOV of the smartphone can result in marker occlusion, and the limited performance of the system, with a maximum of 30 Frames Per Second (FPS), may lead to difficulties in trainees' concentration.

3.3.2 CS WAVE

With the backing of the European Commission, the company CS and the *Agence nationale pour la Formation Professionnelle des Adultes* established the WAVE R&D project in 2002 [64]. The software developed in the scope of this project, CS WAVE, aims to distinguish welding motion skills from complete welding training and provides users with the ability to interact in a virtual environment that is continuously monitored. The virtual environment removes the hazards involved with welding and provides the learner with easy-to-follow visual instructions to assist him in maintaining control of his motion. To utilize CS WAVE, the trainee walks to one of the workstations, then is first exposed to the concepts he must learn, followed by a video demonstrating the proper body orientation for the activity, and lastly trains the welding process in a virtual environment. During training, the learner receives real-time feedback from the simulator. Afterwards, the simulator evaluates the trainee's performance and identifies potential areas for improvement [64]. Experiments with CS WAVE demonstrated that during the introductory period of a trainee's instruction, the system may decrease raw material consumption by 30% and reduce training costs by half, while partially replacing the instructor [64].

3.3.3 ARC+

Montreal-based 123 Certification Inc. developed the ARC+, a welding simulator that has undergone extensive testing, since the early 1990s, and was launched in 2006 [67]. The ARC+ welding simulator is a VR system and web-based teaching facility that mimics multiprocess, multi-material, multiposition, and multipass welding. It consists of an actual welding electrode holding and gun, a helmet-mounted display, a tracking system with six degrees of freedom for hand and head interaction, and external audio speakers. The simulation of welding is based on the rules of physics and twenty years of welding test data from industrial applications [67]. Using a local neural network, the simulation determines the quality and shape of the weld in real-time, depending on the direction, distance, speed of the torch, and depth of penetration. With the use of interactive training modules, the virtual environment depicts the welding procedure and the final weld bead. After welding, the weld quality and recorded process parameters can be evaluated and diagnosed. The instructor can construct a learning curve for each student, and each virtual welding session, to facilitate the learning process [67]. Figure 3.7 depicts a trainee engaging in a training session. In this particular session, the gas tungsten arc welding (GTAW) process is being trained.

Figure 3.7: ARC+ VR training for gas tungsten arc welding (GTAW) [67].

To summarize this section, Figure 3.8 provides a clear analysis of the unique features of the three simulators. This figure illustrates the specific characteristics that each simulator embodies.

3.4 Proposed Classification for the Virtual Reality Welding Simulator

Virtual reality welding simulators offer a diverse range of functionalities. As such, it becomes crucial to select the characteristics to be implemented during the simulator's development, considering the specific objectives of the application. This selection ensures the creation of a well-balanced and cost-effective product that meets the desired goals. This dissertation proposes to classify simulators into three categories: *Minimum*, *Recommended*, and *Advanced*, based on the elements that each level should provide. Each category is assessed based on the characteristics of the simulated welding environment, the feedback offered, and other parameters. Figure 3.9 shows the three categories described as well as their respective characteristics.

The first category, *Minimum*, describes the very minimum characteristics that must be included in a welding simulator. As such, it is the least expensive of the three and may be utilized on devices with lower features, such as mobile phones. This is ideal for individuals who wish to practise at home without needing to acquire expensive equipment. This level stipulates that a VR welding simulator must be able to provide a basic depiction of welding, replicate at least one of the principal welding techniques, and demonstrate the actual functioning of the welding torch and helmet. In addition, it should include a visual feedback system that aids the user with torch travel speed, angle, route, and distance to the weld. It must also include at least one of the main welding positions.

			Mobile VR Welding Kit	CS WAVE	ARC+
Weld Environment		Physics based weld	✗	✓	✓
		Current / voltage control	✗	✓	✓
		Control of the quantity of wire and gas fed	✗	✗	✓
		Four main welding methods	✗	✓	✓
		Simulation of noise and sparks	✓	✓	✓
		Proper operation of the torch and helmet	✓	✓	✓
Feedback	Visual	Torch travel speed, angle, path and proximity to the weld	✓	✓	✓
		Ghost guide	✗	✓	✓
	Gesture	Vibration	✗	✓	✓
		Robot-assisted immersive kinematic	✗	✗	✗
	Auditory	Warnings	✗	✓	✓
		Indications from a trainer	✗	✓	✓
	Post-simulation	Quality	✗	✓	✓
		User performance	✗	✓	✓
		Points to improve	✗	✓	✓
		Muscle activity analysis	✗	✓	✗
		Neural network system for weld analysis	✗	✗	✓
Other Parameters		Four main welding positions	✓	✓	✓
		Allow the user to freely manipulate objects to create new scenarios.	✗	✗	✗
		Controllers and headsets should resemble welding equipment	✓	✓	✓
		Allow students to compete against one another and engage with teachers in real-time	✗	✗	✗

Figure 3.8: An analysis of the distinctive features of the three simulators.

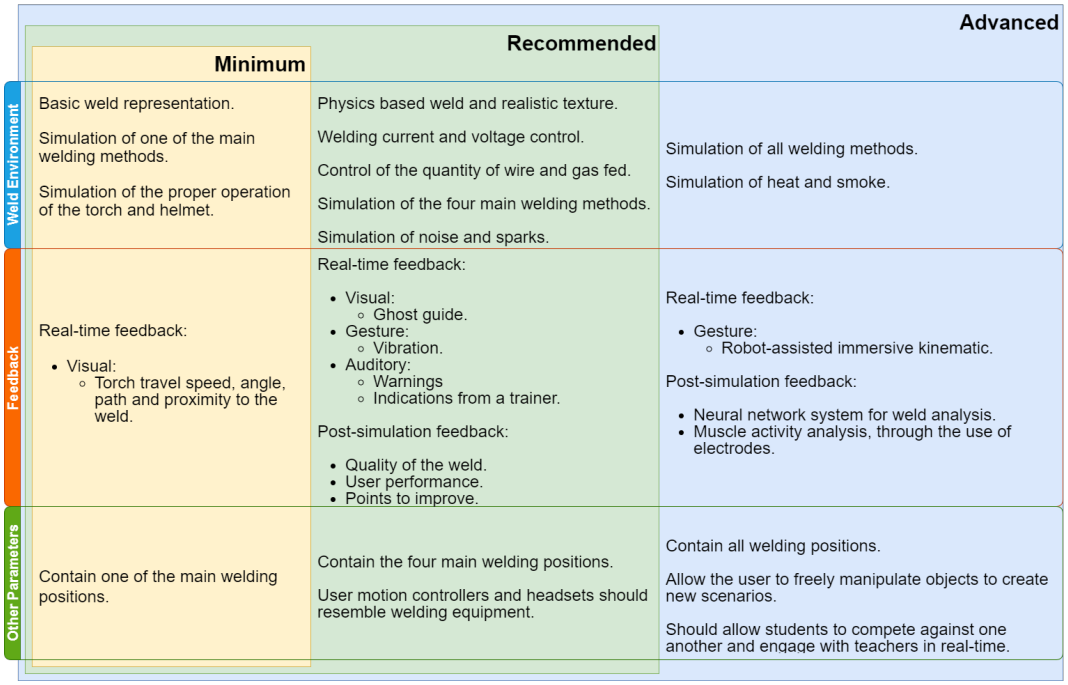

Figure 3.9: Suggested categorisation of VR welding simulators based on their characteristics and functionalities.

The second choice, *Recommended*, is an intermediate answer that schools should strive towards. In comparison to *Minimum*, this renders a realistic-looking weld based on physical principles. In addition, trainees should have the flexibility to manage the device's current, voltage, mode of operation, and gas and wire supply. The simulator should include the three most common welding techniques (SMAW, GTAW and GMAW) and be capable of simulating the resulting noise and sparks. The equipment used to record the user's motions (controllers and headset) should be as similar as feasible to that utilized in the actual welding operation (welding torch and helmet). In terms of real-time feedback, it should have a phantom guide that the student may follow while welding, a vibration mechanism that informs the student when they deviate too far from a desirable parameter, as well as audio instructions and warnings. After the simulation, this system should be able to offer a record that scores the weld's quality, its appearance, and the user's performance. It must also highlight areas for improvement. At this level, the simulator must include at least the four primary welding positions (2F, 1G, 3F and 3G).

Advanced, the third and final level, has the most expensive equipment and software. This is the solution with the most sophisticated technology and the most functionality. This system must support as many welding techniques as possible and imitates the heat and smoke created during welding. Regarding real-time feedback, it should comprise a system that makes use of a cooperative robot arm to

improve students' motor skills, as visible in Figure 3.10.

Figure 3.10: Real-time feedback, cooperative robot arm to improve students' motor skills [68]. The robot guides the trainee's hand along the expert's trajectory.

The suggested method uses high stiffness impedance control to guide the trainee's hand along the expert's trajectory, helping them learn the motion pattern through proprioception. To familiarize the trainee with the expert's force amplitude and direction, the robotic system applies a force to the learner's hand. With this technology, an expert's motor skill can be digitalized and used to teach novices [68]. In the post-simulation feedback section, it should use techniques like neural networks to analyze the weld and electrodes to read the student's muscle activity. This system should include all weld positions [6] and allow trainees to freely interact with a variety of objects in order to generate new welding scenarios. With the advancement of cloud services, the simulator should allow trainees to compete against one another and engage with teachers in real-time, in other simulators.

Regardless of category, all simulators may adhere to the methodology stated by Beck *et al.* [69], which represents the immersion dimensions (narrative, system and challenge) in a 3D scatterplot. The narrative axis represents the storytelling component of the Virtual Reality Welding Simulator (VRWS). It includes instructional design, scenario creation, and the general structure of the learning experience. This axis measures the capability of the system to engage and direct the trainee. The system axis measures the level of immersion and realism within the VRWS. It includes technological aspects such as the quality of imagery, sound, and haptic feedback, as well as the degree of interactivity and presence felt. The challenges axis represents the variety and difficulty of the presented tasks. It involves various levels of difficulty,

variations in welding techniques, and the incorporation of problem-solving scenarios. Figure 3.11 illustrates the three-dimensional space described, encompassing the proposed categories for the welding simulators.

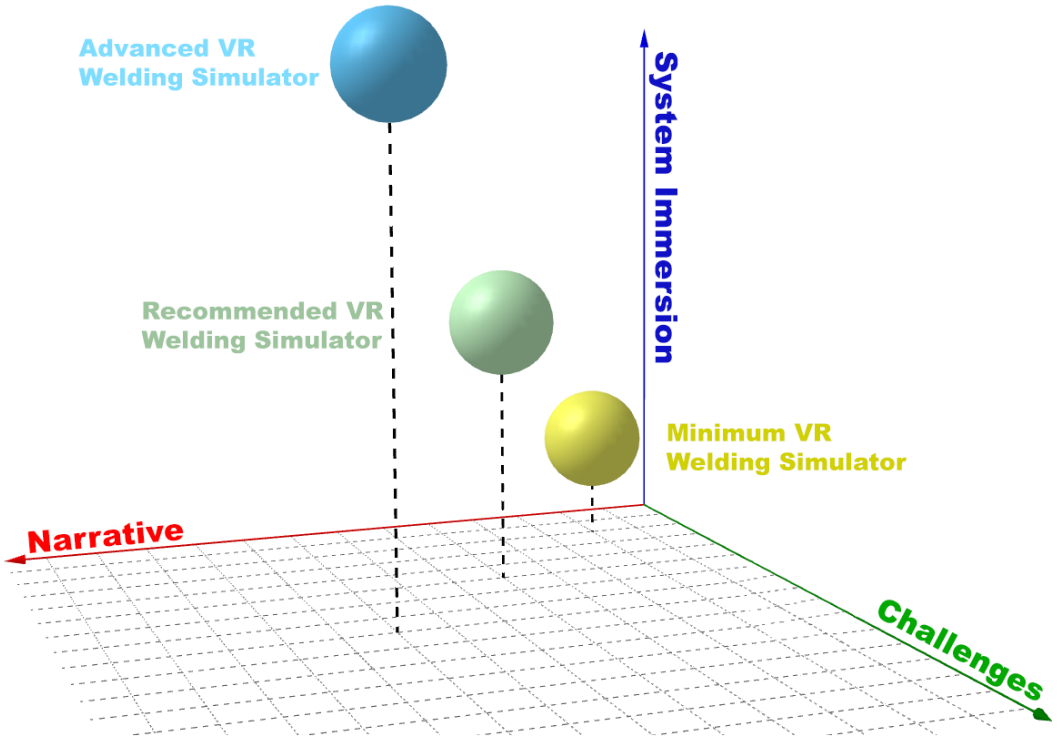

Figure 3.11: Three-dimensional space from Beck *et al.* philosophy [69], and the framework of welding simulators within it.

3.5 Conclusions

The results of the conducted study support the use of VR systems for training novice welders, as they have been found to develop the same cognitive skills as traditional methods. Additionally, VR training has demonstrated greater efficiency in terms of time and resource utilization and has produced welders with comparable, or superior, performance levels to those trained through conventional methods. The simulators have been proven to encourage trainees to improve their outcomes and explore different welding techniques.

The work done so far suggests that there is significant potential for further development in VR systems for welding training. One possible enhancement would be to broaden the range of welding techniques and positions provided in the simulation. The studies revealed a paucity of GTAW and Flux-Cored Arc Welding (FCAW) technique coverage, as well as a narrow number of pipe training positions. On the other hand, the simulators could benefit from a greater focus on narrative to increase trainee motivation. It is also worth noting that, with the advancements in cloud and

edge computing, the simulators should embrace mechanisms that allow trainees and instructors, from different simulators, to engage together. This would enable them to compare their work and compete with each other, fostering a sense of community and healthy competition.

It should be noted that the cost of implementing these solutions can vary significantly. For the *Recommended* category, excluding the simulator license and the required space (2 m by 2 m), the estimated cost in 2023 ranges from 1000 € to 2000 € for the VR system, with an additional 1500 € for a computer to run the simulation.

Chapter 4

Virtual Reality Welding Simulator

This chapter presents a comprehensive examination of the software development approach employed in the construction of a welding simulator. It offers a thorough exploration of the tools, methodologies, and strategies implemented in the project.

The first section, Development Software, commences with an introduction to the development environment, Unity. Subsequently, it scrutinizes the programming languages utilized in the project, specifically C# and High-Level Shader Language (HLSL). The second section, Virtual Reality, provides an overview of the VR equipment used, namely the HTC VIVE Pro 2. It also delves into the virtual reality environment that has been developed. The third section, Fluid Simulator, conducts an in-depth analysis of a Computational Fluid Dynamics (CFD) simulator, providing a clear explanation of it is functioning and emphasizes its crucial significance in replicating welding operations. The fourth section, Parallel Processing, explores the implementation of parallel processing in this project, highlighting its significant influence on improving computational efficiency. Finally, the last section explains the relationship between the various elements of the virtual reality welding simulator.

4.1 Development Software

In contemporary software development, the task of creating applications from scratch has evolved significantly. The availability of powerful game engines, such as Unity,

Unreal Engine, and CryEngine, has streamlined the application development process, particularly for immersive experiences like VR. These engines offer compelling graphics capabilities and are compatible with VR technologies, making them valuable assets for VR application development. Each of these engines has its own distinct advantages, tailored to various preferences and project specifications. Ultimately, the choice of engine is frequently influenced by the user's familiarity, work environment, and community support. Unity was chosen as the primary engine for developing the VR welding simulator in the context of this thesis. The reason for the selection relates to its accessibility, simplicity of learning and a large user community. In addition, the presence of experienced Unity users within the work environment provided invaluable support and expertise, further validating its selection.

In the development of the VR welding simulator within the Unity engine, the project relies on two primary programming languages: C# and HLSL. C# functions as the foundation for the development of the project within the Unity environment. C# is a flexible object-oriented programming language that provides comprehensive support for the development of interactive and aesthetically engaging applications. It is responsible for the implementation of game logic, user interactions, and the application framework as a whole. HLSL, a specialized programming language, is employed in compute shaders, a type of script, in Unity, used to run programs in the GPU. Compute shaders are crucial for maximizing the parallel processing capabilities of modern graphics hardware, enabling sophisticated simulations and graphical enhancements. HLSL provides precise control over graphics rendering and data processing on the GPU, thereby augmenting the VR welding simulator's computational efficiency.

4.2 Virtual Reality

As stated in Chapter 2, there are currently a number of notable hardware solutions that can be used to immerse the user in the VR experience. For this project, INESC TEC provided a set of HTC VIVE Pro 2. The hardware consisted of two controllers, one HMD and four base stations, placed in a square formation, roughly 2 meters squared.

During the year 2020, significant changes occurred in the realm of VR technology inside the Unity platform. These changes are attributed to the development of Unity's Extended Reality (XR) Interaction Toolkit. The toolkit has become increasingly important in the broad field of XR development. It offers a comprehensive set of tools and features designed to accelerate the process of creating VR and AR experiences.

The XR Interaction Toolkit has been designed with a built-in adaptation feature, which ensures interoperability across various XR platforms such as the Oculus Rift, HTC VIVE, and Windows Mixed Reality.

The fundamental principle behind the XR Interaction Toolkit is the distinction between interactions and interactors. Interactions involve a range of activities that may be performed inside a virtual world, including basic movements such as grasping, touching, and pushing. In addition to these interactions, there are interactors, which refer to the entities or mechanisms that start and enable these activities.

The XR Interaction Toolkit enhances the repertoire of developers by providing a wide array of interaction components, such as grab interactables, teleportation systems, and interface interaction tools. These components are fundamental elements used in the construction of the XR environment.

The first step in incorporating the XR Interaction Toolkit into a Unity project is obtaining the toolkit from Unity's Asset Store. The subsequent procedures include the importing of the XR Origin GameObject, which functions as the central point for XR device setup. The current GameObject is responsible for coordinating the configuration process of the HMD camera, as well as the left and right controllers. Figure 4.1 depicts the XR Origin GameObject, for the HTC VIVE Pro 2 HMD and controllers. The toolkit is designed to support a wide range of XR hardware setups, and freely available online resources provide pre-configured mappings for commonly used devices. Nevertheless, in some cases, specialized or tailored hardware arrangements may need the manual tuning of mapping settings in order to achieve compatibility. As detailed later in this section, manual mapping is required to enable the use of the HTC VIVE Tracker.

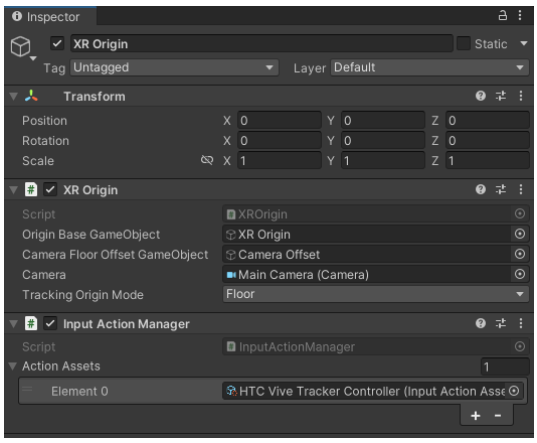

Figure 4.1: Final configuration of the XR Origin GameObject

After establishing the hardware base, the following logical progression involves the integration of interactive features inside the XR environment. The efficiency of this procedure is enhanced by the use of the XR Grab Interactable script, which is a pre-existing component that can be implemented on virtual objects. This script

enables developers to enhance objects with interactive functionalities, including activities such as grasping and manipulation, as well as more intricate user interface interactions.

For the testing of the VR environment, a small set illusive to the welding applications, depicted in Figure 4.2, was created. The virtual environment consists of two workbenches, each equipped with an orange cube where welding operations may be conducted. Furthermore, there's a pink cube equipped with the XR Grab Interactable script, allowing the user to engage with it in an interactive manner. The scenario also includes key welding instruments, such as a cutting plier, a welding mask, and a MIG/MAG torch. These instruments possess a comparable script to that of the pink cube, enabling the user to manipulate them.

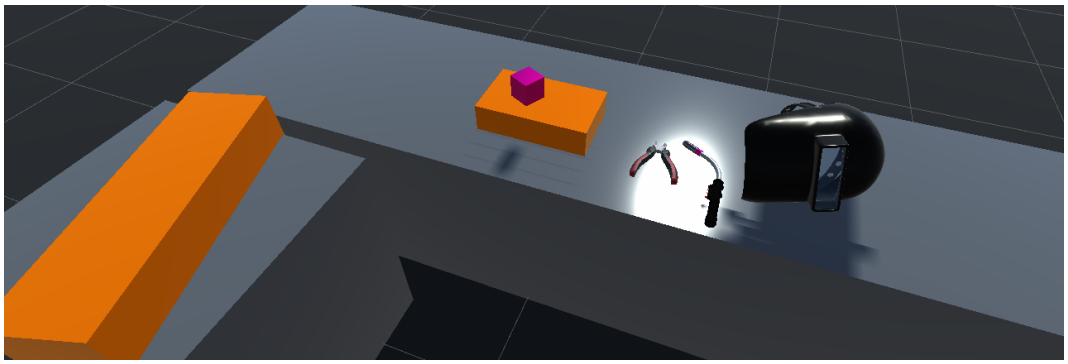

Figure 4.2: VR welding environment developed.

The cutting plier offers a unique feature, enabling the user to trim excess wire from the welding torch. An animation was programmed to simulate the cutting process, that has been illustrated in the Figure 4.3 a). The welding mask is designed to be worn by the user, mimicking the act of putting on a real mask when brought close to the head, Figure 4.3 b). It contains a script with an animation depicting the mask's movement and simulating the behavior of the mask's glass closure under intense light conditions, Figure 4.4.

The MIG/MAG torch is capable of simulating the operation of a real MIG/MAG torch. Users can initiate welding by pressing the torch's button, causing wire to dispense from the torch's tip, Figure 4.3 a) upper case. If the wire exceeds the desired length, users can employ the cutting pliers to trim it, Figure 4.3 a) bottom case.

Figure 4.5 displays a person testing the welding simulator, as well as their viewpoint inside it.

Furthermore, a basic Smoothed-Particle Hydrodynamics (SPH) simulation for welding is currently integrated into this environment. This can be seen in the figures above. However, as discussed in the following section, this simulation will be replaced by a more realistic and performance-oriented alternative.

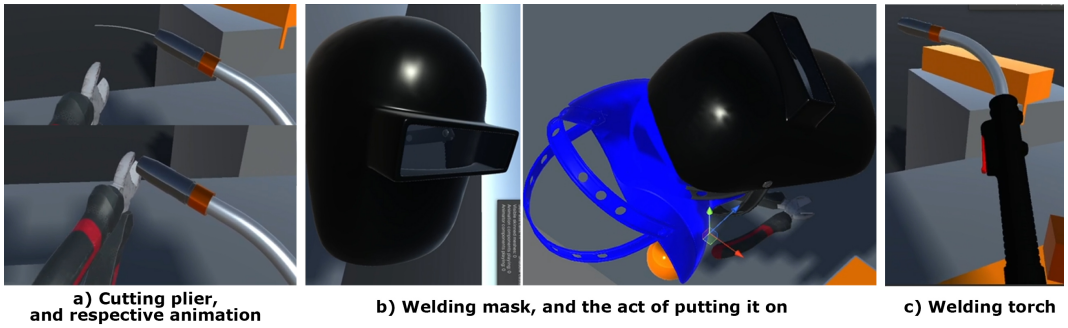

Figure 4.3: Tools developed for the VR welding simulator (video available at [70]).

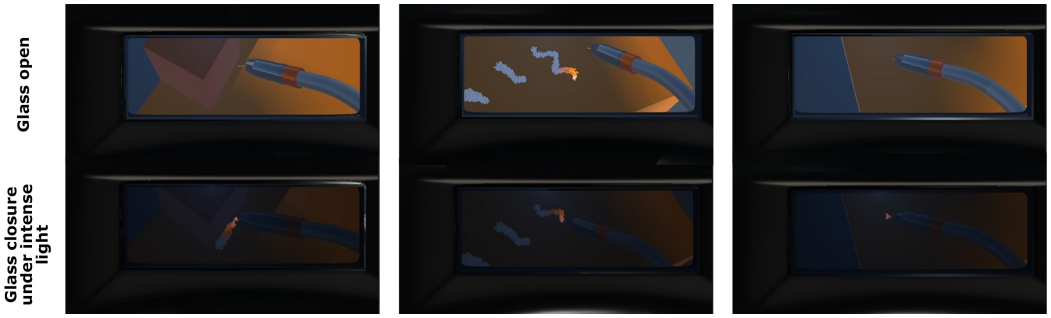

Figure 4.4: Welding simulation, and mask's glass closure under intense light conditions (video available at [70]).

Figure 4.5: A person testing the welding simulator, as well as their viewpoint inside the simulator (video available at [70]).

As suggested in Chapter 3, enhancing the simulation's immersion involves the utilization of a real welding torch as the controller for the simulator. Several approaches can achieve this, ranging from custom-made controllers to actual torches equipped with motion-tracking devices. In this project, the latter approach was chosen, with the aim of equipping a real welding torch with an HTC VIVE tracker. These trackers can be mounted onto objects and, when used in conjunction with HTC VIVE base stations, transmit the object's movement to the virtual environment. Figure 4.6, sourced from the HTC VIVE tracker manual [71], provides two examples of a tracker mounted in pistols.

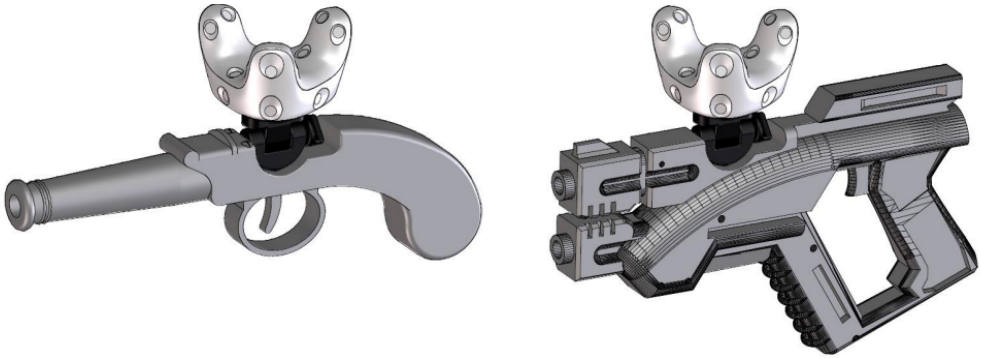

Figure 4.6: HTC VIVE tracker used for object tracking [71].

These trackers come equipped with a set of connectors that developers can utilize to control their custom controllers. As depicted in Figure 4.7, sourced from the tracker's manual, there is one digital output pin, which can, for example, be employed to trigger a light or, perhaps, a vibration system, one ground pin, and four digital inputs. Of these four, the first has the capability to double as a power input pin for charging the device.

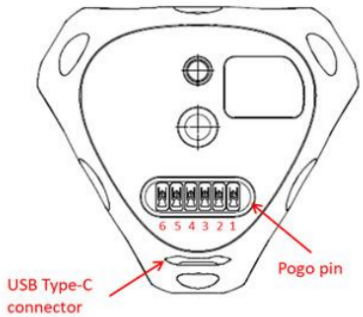

Pin no.	Type	Description
1	Digital output	General purpose output pin
2	GND	Ground
3	Digital/Power input	1. General purpose input pin: Internal pull up resistor to VDD, Active -low (Grip button) 2. Power input pin
4	Digital input	General purpose input pin: Internal pull up resistor to VDD, Active -low (Trigger button)
5	Digital input	General purpose input pin: Internal pull up resistor to VDD, Active -low (Trackpad button)
6	Digital input	General purpose input pin: Internal pull up resistor to VDD, Active -low (Menu button)

Figure 4.7: HTC VIVE tracker pinout [71].

As previously mentioned, when employing custom controllers, manual mapping becomes necessary for correct operation. In this case, there are only three parameters that require configuration: one for mapping the controller's position, one for its rotation, and one for the trigger button. For each of these parameters, the user needs to define the action type, which can be set as either a value or a button[1], and the control type, if the chosen action type is value. For the three parameters mapped, the action type selected was value. As for the control type, for the position it was set as a Vector3, to store the coordinates in all three axes, for the rotation it was set as a Quaternion, to store the rotation in each axis, and for the trigger it was set as Analog, allowing the reading of the pressure applied to the button. In addition to the action and control types, the developer must specify the correct data path from which the information should be retrieved. Figure 4.8 displays the window used to configure these parameters, with the respective data source path displayed below each parameter (position, rotation, and trigger). When a parameter is selected, a subsection appears on the right, allowing for the definition of action and control types.

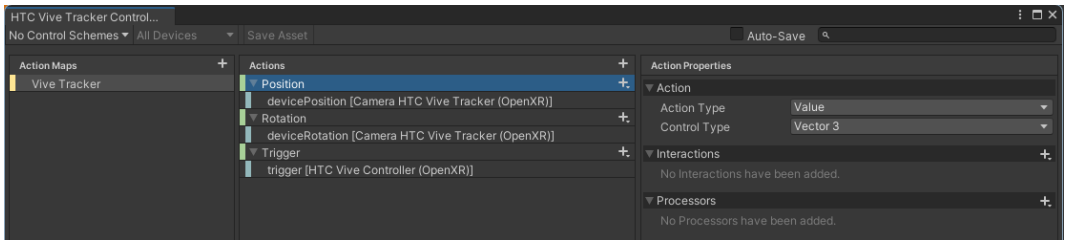

Figure 4.8: HTC VIVE tracker mapping window.

4.3 Fluid Simulator

In a welding simulator, the central element is the weld itself. Therefore, developing an accurate physics-based representation of the weld is imperative. A weld typically undergoes two primary states: a fluid-state, resembling a viscous substance, like honey, when subjected to high temperatures, and a solid-state after cooling. Consequently, creating a fluid simulator is the most suitable approach for simulating a weld. This fluid simulator possesses a unique characteristic, it must account for the temperature of the weld, allowing it to transition between liquid and solid states accordingly.

As previously stated in Chapter 2, there are three primary architectures for fluids simulations. Due to its ease of implementation, a Smoothed-Particle Hydrodynamics (SPH) simulation was utilized in this project's initial approach, that can be seen in

[1]The action type is only set to button when the value returned, by the controller to that parameter, can only be one or zero.

Figure 4.9. As stated, SPH simulations are rooted on the behaviour of the fluid's particles. By designating a RigidBody component to each one of them, it is possible to use Unity's built-in physics system to simulate a realistic physical behaviour. This physics engine is capable to simulate a particle action when subjected to external forces, such as gravity or drag. In addition, it can be used to simulate collisions. In order to use the RigidBody component, the mass and frictional force of the particle need be configured [72]. The first can be calculated using the welding material density and the particle volume, as per the second, by applying the Stokes' Law its possible to determine a particle frictional force based on the fluid viscosity [73]. In addition to the RigidBody component, each particle requires a C# script to simulate the cohesive forces between particles [74].

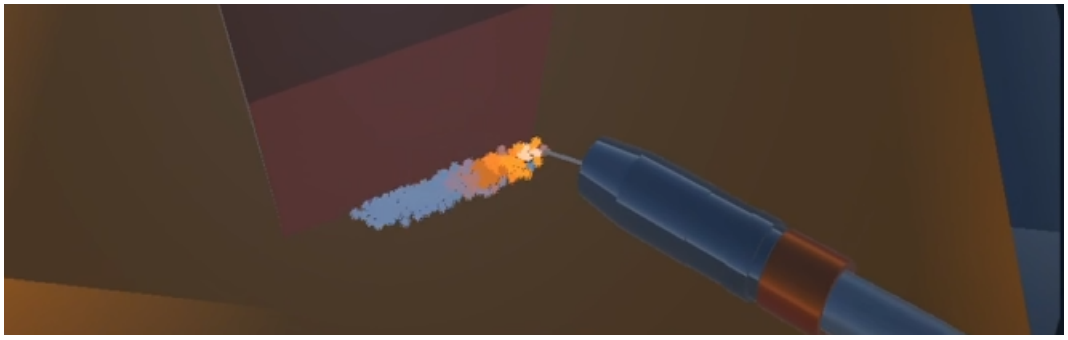

Figure 4.9: SPH welding simulation (video available at [75, 76]).

This approach has proved capable of creating horizontal welds and correctly conveying the temperature of the material. However, it had problems creating vertical welds, as it was unable to support itself, and always fell to the bottom. In addition, the visual quality of the material was poor. This could be compensated for by decreasing the particle size, which in turn would lead to an increase in the number of particles and the computational cost. This was the point that proved to be the most disadvantageous in SPH. Its high number of particles resulted in simulations of less than 10 FPS, breaking the sense of immersion[2].

Attempting to enhance simulation quality and efficiency, a Computational Fluid Dynamics (CFD) architecture was employed. This type of simulation is known for its versatility and accurate representation of physics, making it well suited for engineering and scientific analysis. Due to the complexity of these simulators, the implementation was broke down in three parts, the grid, the Navier-Stokes equations (fluid equations) and the fluid render. This section will follow that order to expose the fluid simulator developed.

[2]As a point of reference, in order to maintain the sense of immersion, the simulator must run at a minimum of 30fps [57].

4.3.1 Grid

As previously discussed in Chapter 2, CFD operates within a grid structure, with each cell storing information about fluid properties such as velocity, density and temperature at those specific points. Thus, the initial step in developing this kind of fluid simulator involves creating the grid.

In many scenarios, the shape and dimensions of the grid remain fixed throughout the simulation. However, for the scope of this thesis, such an approach would prove impractical. The workspace is vast, and using a static grid would require an exceptionally large grid size, imposing a considerable computational burden on the system. To address this challenge, two primary solutions were considered. The first solution involves the use of an Octree data structure. This approach begins with a single cell that encompasses the entire workspace. As the user performs welding actions, the cell dynamically subdivides, increasing resolution in the region of interest. However, this technique has a drawback, the process of reverting divided cells incurs a substantial computational cost. Conversely, the second method employs a dynamic grid that forms as the worker welds. This approach offers the advantage of a grid that exists solely in regions where welding is taking place. Nevertheless, it faces two key challenges, cell identification and grid traversal, primarily because the cells are not created sequentially, and they are not bound by specific spatial constraints. In other terms, there's no direct way to identify neighboring cells or to correlate cell identification with their spatial coordinates. After evaluating and conducting tests on the two grid options under consideration, the dynamic grid was selected for implementation due to its relative ease of implementation. In terms of performance, for the same number of cells, both networks scored similarly. In order to address the specific challenges associated with this grid type, in addition to the previously mentioned data stored in each cell, it becomes necessary to store the identification of the six adjacent cells, the coordinates of the cell center, and a boolean value representing whether the cell is a border or not. Figure 4.10 illustrates the three grid types. The first is the regular grid, where all cells have uniform sizes. The second is the octree grid, which provides higher resolution to cells containing objects. Lastly, the third is the dynamic grid, where all cells are of uniform size but are only created in areas where welding has occurred.

The dynamic grid operates by initially creating a cell at the welding starting point, Figure 4.11 a). Subsequently, the system generates a cluster of cells that completely enclose the initial cell, Figure 4.11 b). The number of cells generated depends on the selected resolution. For instance, when the resolution is set to the minimum (three), each fluid cell is surrounded by a 3x3x3 cube of cells (a total of twenty-six). During the creation of each cell, the programme attempts to identify

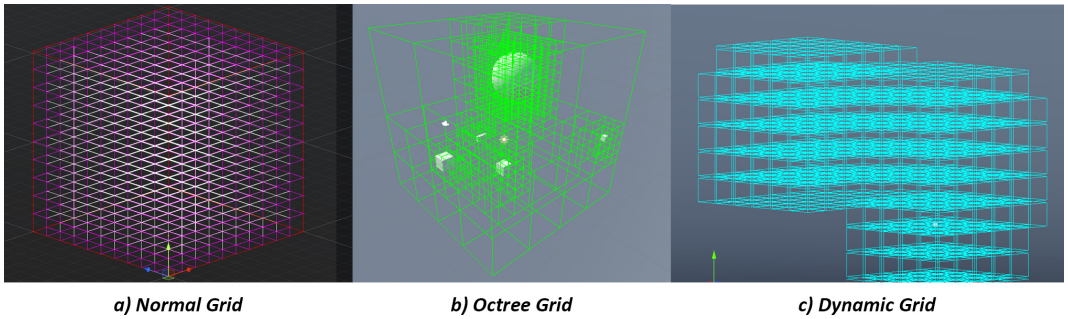

Figure 4.10: The three grid types tested for this project

neighbouring cells. If all neighbors [3] are found, the cell is designated as a fluid cell (cyan). If at least one neighbour is missing, the cell is labelled as a border cell (magenta). As the user navigates through the grid, whenever they enter a border cell, the system automatically generates new cells to cover it, thus removing its border cell status and converting it into a fluid cell, Figure 4.11 c) and d). Moreover, the cell's neighbour list is updated, as well as the lists of cells that might be adjacent to the newly created cells.

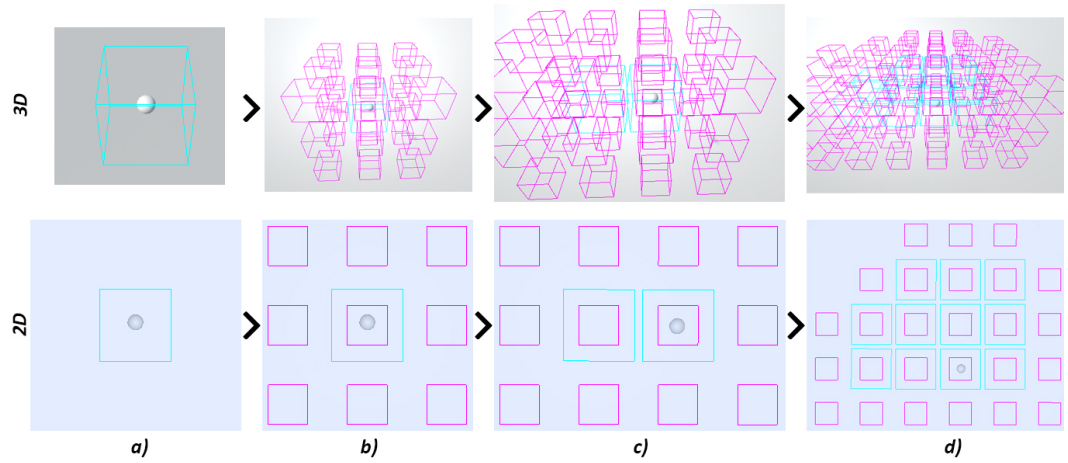

Figure 4.11: Dynamic grid creation: a) Initial cell; b) Neighbor formation; c) User shifts one cell right, updating the grid; d) Grid status after several user movements.

After the development of the grid, two crucial tests were conducted. The first test ensured that newly generated cells received the correct identification numbers and did not overlap with existing cells. Figure 4.12 a) illustrates the conducted test, with each cell assigned a color corresponding to its identification number. Initially generated cells are marked with a yellow hue, transitioning to a reddish tone as the cell numbers increase. As depicted in this figure, when the user's movement crossed itself, in two instances, the cells were generated correctly. In these cases,

[3]The system considers only the cells directly adjacent to a given cell as its neighbors, totaling six neighboring cells (front, back, top, bottom, right and left).

the system recognised the presence of existing cells in that location and prevented new ones from being created. The second test was conducted to ensure the accurate identification of border cells. Since this project operates with a dynamic grid, the border conditions are continually changing. Therefore, it is crucial that all border cells are correctly identified. As depicted in Figure 4.12 b), each cell with at least one missing neighbour is designated as a border cell (magenta).

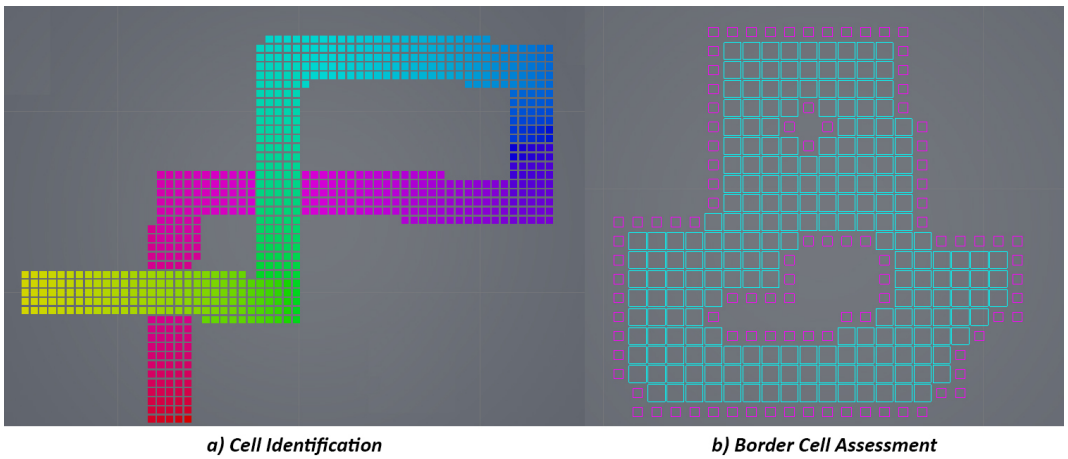

Figure 4.12: Tests conducted to assess the dynamic grid: a) Cell identification (video available at [77]); b) Border cell assessment.

4.3.2 Navier-Stokes Equations

CFD is based on solving the Navier-Stokes equations, which mathematically characterize the conservation of mass, momentum, and energy within a fluid. These equations can be decomposed into two primary equations [78].

The first equation, often referred to as the momentum equation, is represented by Equation 4.1[4]. It denotes how the velocity changes over time and can be divided into three terms: *advection*, *diffusion* and *external forces* [57, 78].

The first term, *advection*, represents how the velocity, $\mathbf{u}$, carries it self over time. In other terms, the fluid velocity is responsible to transport "matter" along with the flow. This "matter" can range from physical objects to fluid properties, such as density and temperature. Furthermore, just how the velocity carries this properties, it can also carry it self. It is mathematically expressed as: $-(\mathbf{u} \cdot \nabla)\mathbf{u}$. The second term, *diffusion*, demonstrates how the fluid's viscosity, denoted as ν, influences its velocity. Viscosity quantifies a fluid's resistance to flow, resulting in the diffusion of the fluid's momentum and, consequently, its velocity. This term can be express as: $\nu\nabla^2\mathbf{u}$. The third term, *external forces*, encompasses all the external forces that

[4]Since $\mathbf{u}$ and $\mathbf{F}$ are three-dimensional vectors, Equation 4.1 can be decomposed into three equations, one for each axis.

are applied to the fluid. It consists of forces such as gravity, wind forces, and those induced by human activities. These forces are denoted as a vector **F** [57, 78].

$$\frac{\partial u}{\partial t} = -(u \cdot \bigtriangledown)u + v \bigtriangledown^2 u + F \tag{4.1}$$

The second equation, represented by Equation 4.2, is known as the conservation of mass equation. It describes the evolution of the fluid mass over time. Similar to the first equation, the structure of the second can be divided into three terms. This similarity is an important characteristic, as it allows for the utilization of the same solver for both equations. The key difference between the two equations lies in the physical property they address. The first equation focuses on the velocity field, denoted as **u**, and its influence on fluid flow. In contrast, the second equation addresses the behaviour of the fluid mass using the density field, ρ. This equation introduces two new variables, κ, that quantifies the density diffusion, and **S**, that encompasses all sources or sinks of density [57, 78].

$$\frac{\partial \rho}{\partial t} = -(u \cdot \bigtriangledown)\rho + \kappa \bigtriangledown^2 \rho + S \tag{4.2}$$

In the above equations, the symbol ∇ is known as the *nabla* operator. For the mentioned equations, this operator has two different applications. It works as the divergence operator, in $\mathbf{u} \cdot \nabla$, and as the Laplacian operator, in $\nabla^2 \rho$.

In order to facilitate the digital implementation of the Navier-Stokes equations, they are often divided into three functions, each of which is responsible for solving one of the terms mentioned above [57]. However, there are studies [79, 80, 81] that solve all three terms in one function, seeking to improve the veracity of the simulation. Although, this leads to a higher computational cost.

The first step to solve the Navier-Stokes equations is the *diffusion* function, that plays a pivotal role in achieving equilibrium within the system. This phase involves the propagation of changes introduced to individual cells throughout the simulated fluid domain. Whether these changes pertain to material deposition, alterations in velocity, or temperature adjustments, the *diffusion* process seeks to homogenize these modifications across adjacent cells. By doing so, the system strives to establish a harmonious distribution of attributes within the simulation space. A simple example of the *diffusion* step can be observed when a drop of ink is applied to a bowl of water. After a few moments, the ink gradually disperses and becomes fully integrated into the surrounding water.

In practical terms, the *diffusion* step operates by traversing through every cell within the grid. During this iterative process, for each value contained within a cell, the system computes the average of its neighboring cells' values. Subsequently, each value within the cell is updated, taking into account both the calculated average of neighboring values and the timestamp of the simulation. This procedure ensures that

the system iteratively tends toward a state of equilibrium. Equation 4.3 showcases the general equation used to calculate the new diffused value. The video available at [82] showcases the test done to this function.

$$x = x_0 + (x_{NeighborAverage} - x_0) * DiffusionRate * \Delta t \tag{4.3}$$

After solving the *diffusion* step, the focus moves to the *advection* phase. This phase is responsible for moving the characteristics of a cell along the simulated fluid domain, which entails the propagation of fluid properties, such as velocity, temperature, or substance, governed by the fluid's inherent velocity field. The fundamental principle of advection is the conveyance of matter by the fluid itself, something that can be seen, for example, as a river that carries leaves along its current.

As the *advection* stage is related to the transport of a cell's characteristics, one can imagine each cell as a particle. A straightforward approach to execute this step involves updating the grid by virtually relocating each particle according to the velocity of its respective cell. In other terms, simply advance the position, $\mathbf{r}$, of each particle along the velocity field by the distance it would cover in a time step, Δt, which could be achieved with Equation 4.4.

$$r(t + \Delta t) = r(t) + u(t) * \Delta t \tag{4.4}$$

However, this strategy has two major drawbacks. First, simulations employing explicit methodologies for advection encounter instability when subjected to substantial time intervals or when the velocity magnitude ($\mathbf{u}(\mathbf{t})$) exceeds the dimensions of a single grid cell. Second, there is a distinct concern regarding the implementation on GPUs. Using this method, the system would modify a cell that is distinct from the initial cell. In the context of parallel processing, this disparity would result in a concurrency issue.

Stam [83] found a solution by inverting the problem and using an implicit method. Instead of using a method of advection that involves calculating the displacement of a particle within the current time step, he traced the particle's path from each grid cell to its previous location and then copied the values associated with that position onto the initial grid cell. This method can be readily implemented on the GPU, and as demonstrated by Stam, it exhibits stability across diverse time steps and velocities. This process can be accomplished through the implementation of Equation 4.5.

$$q(x, t + \Delta t) = q(x - u(x, t) * \Delta t, t) \tag{4.5}$$

The implementation of this step in a standard grid is straightforward. Given a starting point (Q) and velocity ($\mathbf{u}$), identifying the previous cell (ID_0) is simple, as cell identification directly corresponds to a spatial position. However, for a dynamic

grid, locating the antecedent grid cell, from which values must be averaged, poses a significant challenge. As mentioned earlier, there is no direct correlation between cell identification and spatial position due to the non-sequential nature of the cells. Figure 4.13 illustrates the idea behind the advection step.

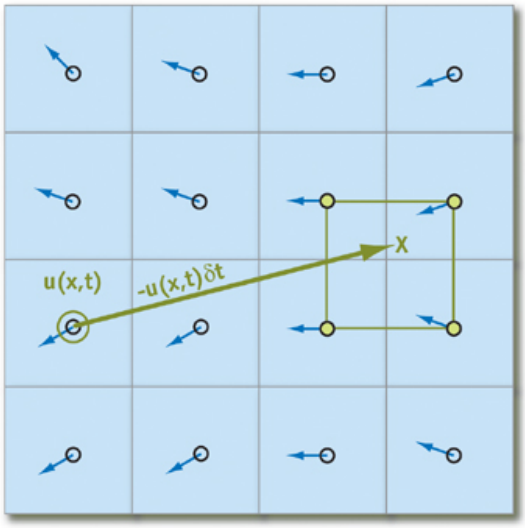

Figure 4.13: Advection function work principle [57].

In the initial approach, the system computed the previous position (Q_0) and then iterated through each cell until it found one containing this point. However, this method imposed a substantial computational burden on the system.

The second strategy involved drawing a line between Q and Q_0. The system then determined the intersection of this line with the current cell, providing the direction to the next cell. This direction was utilized to ascertain the ID of the subsequent cell, since each cell retains the IDs of its adjacent neighbors. This process continued until the cell containing Q_0 was identified. Although this new method proved significantly more effective by traversing only the cells along the velocity path, it had a notable drawback. It relied on calculating intersections by instantiating virtual cubes. If this strategy was implemented with parallel processing, multiple cubes could be created at the same location or along the same line, resulting in inaccurate calculations.

Building upon the second attempt, a third strategy emerged, replacing intersections with inequality equations. This phase is governed by a total of six inequality equations, one for each direction. Figure 4.14 depicts only the three positive regions and their corresponding inequalities equations for ease of visualization, with the remaining three corresponding to the negative counterparts. After computing Q_0, the system subtracted Q to yield three distances (x, y, and z). These distances, in conjunction with the inequality equations, were then used to determine the direction of the next cell and, consequently, its ID. This process continued until the system

reached the cell containing Q_0. This solution proved to be the most efficient and effective option.

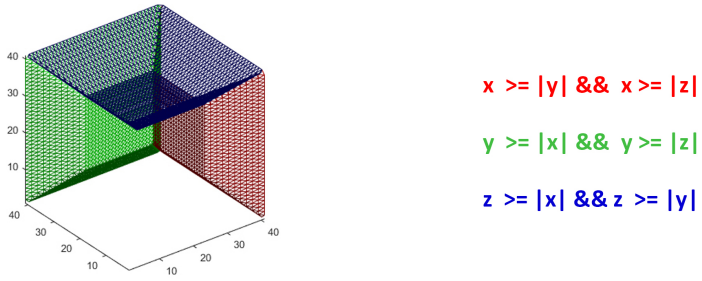

Figure 4.14: The inequality equations for the advection function, and the respective representation in 3D space.

This last solution exhibited a problem. If Q_0 was to be positioned outside of the grid or in a border cell, the outcomes would be inaccurate. In order to mitigate this scenario, before stepping into the next cell, in the path, the algorithm checks if it wasn't a border. In the event that the cell assumes the role of a border, the software would proceed to recompute the value of Q_0, designating it as the location at where the line intersects the border, and conclude the search process.

Following the identification of Q_0 and ID_0, the system is required to compute the average of the neighboring values. In order to carry out this task, it is necessary to identify the nearest cells and determine their respective weights. The simplest methodology for determining the nearest cell is to think of ID_0 as partitioned into eight distinct areas, and then ascertain in which one Q_0 is located. This process is as simple as comparing Q_0 to ID_0 center coordinates. After determining the eight closest cell to Q_0, the system proceeds to calculate the weight of each one. Knowing that each cell has the same size, the weights can be determined in function of the distance of Q_0 to ID_0 center. Each axis will yield two weights, one for the portion of the Q_0 and one for the portion of the neighbouring cell. To enhance clarity, the notation W_{0_x}, W_{0_y} and W_{0_z} are used to represent Q_0's weights, while W_x, W_y and W_z refer to the weights associated with neighboring cells. Below is the system of equations 4.6 for computing these weights.

$$\begin{cases} W_n = |ID_{0_n} - Q_{0_n}|/Cell_{Size} \\ W_{0_n} = 1 - W_n \end{cases} \tag{4.6}$$

Once the weights for each axis have been calculated, these numbers are utilized to determine the weight of the neighbouring cells. For example, the weight of Q_0 is derived from the product of W_{0_x} by W_{0_y} and W_{0_z}, while the weight of its neighbor along the x-axis is determined by multiplying W_x by W_{0_y} and W_{0_z}. To make it simpler to visualize how the implemented *advection* function operates, the z-axis

component has been removed, resulting in Figure 4.15. The cell with a white circle is the cell in study (ID). The red line in the graph represents the path of the particle to its previous cell (ID_0), and at the end, in white, is a small dot that represents Q_0. The orange wireframe rectangle delineates the four closest cells to Q_0. In green, red, cyan and yellow are represented the weights of the neighbours, the exact value of each one can be seen in the footnote of the image, as well as the ID_0 number.

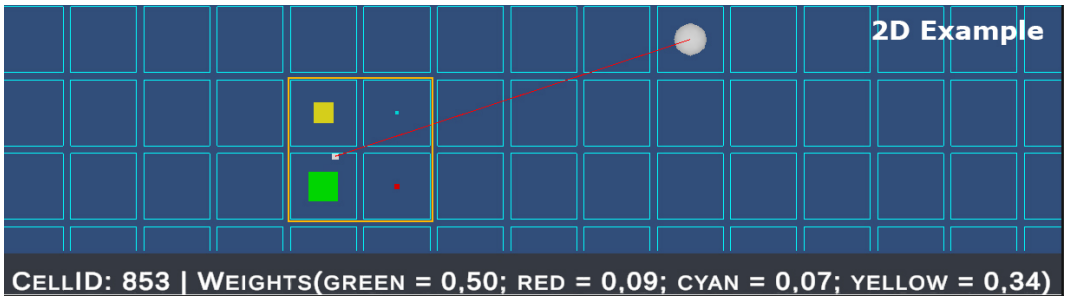

Figure 4.15: The implemented *advetion* function, with the z-axis component removed, for ease of visualisation.

Figure 4.16 illustrates a special advection scenario. In this example, Q_0 is positioned adjacent to a border. Consequently, the system only takes into account two neighboring cells, as the other two belong to the border. In this specific case, the weight of W_y equals zero, while W_{0_y} is set to one.

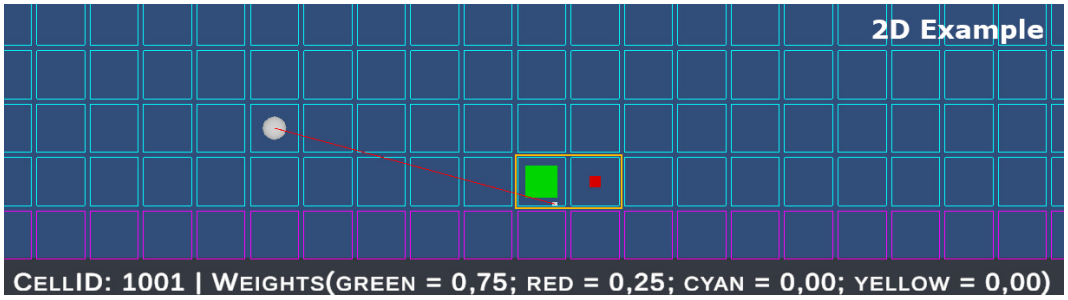

Figure 4.16: Special advection scenario, Q_0 is positioned adjacent to a border.

The last step in the advection function involves computing the value (q) passed to the current cell. This calculation relies on the previously determined weights, the prior values of the neighboring cells (q_{0_n}), the value from the cell under study (q_0), and the time step (Δt). This process is outlined in the Equation 4.7. The video available at [84] showcases the test done to this function.

$$q = q_0 + (\sum(q_{0_n} * W_n) - q_0) * \Delta t \tag{4.7}$$

The next step, following the solution of *advection*, involves the implementation of the *projection* function. Its primary objective is to maintain the incompressibility of the fluid's velocity field. Incompressibility implies that the mass of the fluid

within a specific region remains constant over time. When external forces act on a fluid, they can create regions of higher or lower pressure. As a result, fluid particles tend to move from areas of high pressure to areas of low pressure, striving to avoid compression or rarefaction. For instance, when water is pushed into an area, causing an instantaneous increase in pressure, the particles within it tend to displace themselves from regions of higher pressure to those of lower pressure, to avoid compression. Similarly, when water is withdrawn from a zone, creating a lower pressure, particles tend to be drawn towards that point. To ensure the incompressibility of the fluid, the projection step compensates for regions where fluid cannot be easily pushed or removed due to pressure variations. This compensation is done by modifying the velocity field.

As Stam [83] stated, according to the Hodge decomposition method, a velocity field is composed of an incompressible field and a gradient field. Thus, to obtain the incompressible field, one can simply subtract the gradient field from the current velocity field. This process can be seen in Figure 4.17.

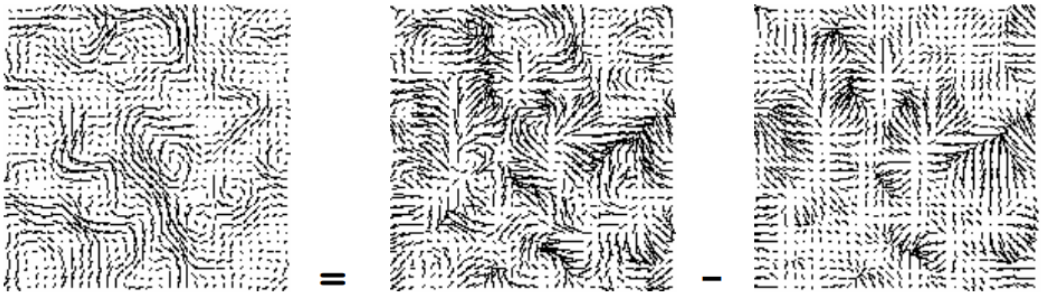

Figure 4.17: The velocity field is the sum of an incompressible field and a gradient field, as Stam [83] stated.

The gradient field, commonly known as the gradient field of a scalar quantity, is a useful tool in mathematics and physics. It indicates the direction and rate of change of the scalar quantity in three dimensions. The gradient at a specific cell points in the direction where this quantity increases most rapidly, and its value represents the rate of change in that direction. It can be used to characterize the spatial variation of a scalar quantity, such as temperature, pressure, or density, in a specified domain. For instance, the pressure gradient field indicates the direction and magnitude of the greatest pressure change within a fluid.

In order to obtain the gradient field, first, it is needed to calculate the divergence field. Divergence measures the rate at which fluid is either accumulating (positive value) or depleting (negative value) at a given point in the flow. A zero divergence indicates that there is no accumulation or depletion of fluid mass, which is a key requirement for an incompressible flow. The divergence (div) can be calculated by summing the divergences along each axis, as Equation 4.8 presents.

$$div = div_x + div_y + div_z \tag{4.8}$$

A velocity vector can be decomposed along the three Cartesian axes. These components are typically represented as u for the x-axis, v for the y-axis, and w for the z-axis. When computing divergence, only the neighboring velocity components aligned with the axis of the cell under consideration are taken into account. For example, when determining the x-axis divergence component (div_x), exclusively the x-axis components (u) of the adjacent cells along that axis (right and left neighboring cells) are considered. As illustrated in Figure 4.18, these specific components are the only ones exerting influence over the flow entering or departing from the cell along the corresponding axis. As can be seen, the divergence function takes in a field of vectors and returns a field of scalars. This function is commonly referred as an operator.

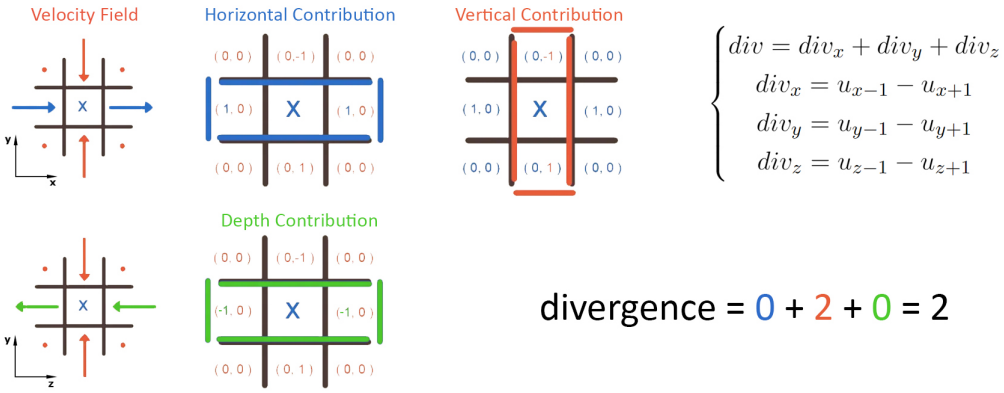

Figure 4.18: Divergence calculation.

In order to implement an incompressible fluid the divergence needs to be zero. In a case with too much inflow, where the divercence is bigger than zero, the system cannot simply change one velocity in order to expel the excess of flow. Instead, it must divide the divergence value for the number of neighbours, and add or subtract, according to the neighbour direction, the resulting value. Figure 4.19 illustrates this process.

In order to ensure incompressibility in the fluid simulation, it is crucial to maintain a divergence of zero. In situations when there is an excessive influx that disturbs the equilibrium, resulting in a non-zero divergence, the system cannot modify just one velocity component, since this does not accurately represent the expected fluid behavior. In this scenario, the system is required to allocate the surplus divergence value among the adjacent cells, modifying it by means of addition or subtraction, depending on the orientation of those adjoining cells. The technique is shown in Figure 4.19.

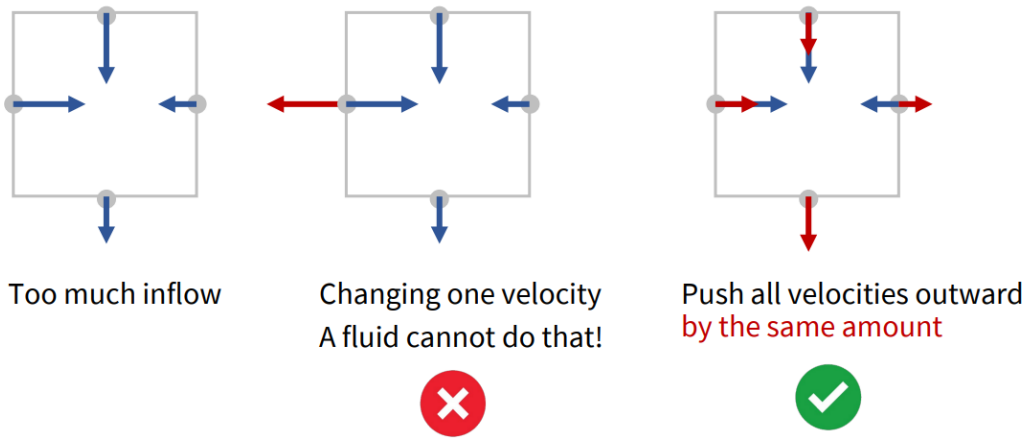

Figure 4.19: Forcing incompressibility In a case with too much inflow.

The process of resolving incompressibility is an iterative method. When the system enforces the incompressibility of velocities in the vicinity of a cell, it requires a further computation of the adjoining cells to verify their incompressibility. The aforementioned repetitive procedure continues until a condition of equilibrium is attained. There are many iterative methods available for solving equations, including conjugate gradient and multigrid approaches [85, 86, 87]. This project utilizes the Jacobi iteration technique due to its simplicity and ease of implementation [88]. One drawback associated with this approach is its very sluggish rate of convergence. Consequently, achieving error minimization often requires a span of 40 to 80 iterations. It is not recommended to have less than 20 iterations, since this might lead to the emergence of visible flaws. Increasing the number of repetitions results in the generation of more intricate vortices and improves the overall precision, but at the expense of longer computing time. In order to reduce the need for a large number of repetitions, the overrelaxation approach may be used. This methodology entails the multiplication of the divergence by a scalar coefficient ranging from one to two, but it is frequently set as 1.9 [88, 57].

One of the incompressible velocity field achieved using the constructed function is shown in Figure 4.20.

4.3.3 Fluid Render

Following the implementation of the grid structure and the computation of the Navier-Stokes equations, the next step in the development of a fluid simulator is the construction of a rendering function to visualize the data contained in the fluid grid. Over the years, programmers have devised numerous techniques for transforming data into 3D objects or other rendering-friendly formats. These techniques have evolved to accommodate the diverse requirements of computer graphics and simulations. Some of the prominent techniques and approaches include the utilization of a

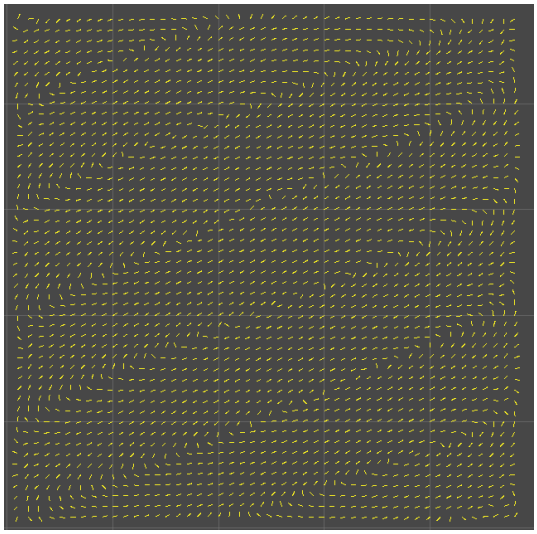

Figure 4.20: Incompressible velocity field.

particle system [89], surface reconstruction algorithms [90], volumetric renderings **??** or the marching cubes algorithm [91].

For this project, the best approach is the implementation of a marching cubes algorithm [91]. It is a remarkable technique for reconstructing 3D surfaces, and it is extensively used for the visualization of scientific data and computer graphics. In addition, as will be explained in this section, the marching cubes algorithm is ideally adapted for CFD simulators.

William E. Lorensen and Harvey E. Cline [91] introduced the marching cubes algorithm in 1987 for processing medical databases comprising 3D information related to human physiology. This ground-breaking algorithm was designed to convert these complex 3D medical datasets into comprehensive 3D models, thereby revolutionizing the field of medical imaging and visualization. Figure 4.21 depicts some of the results achieved these authors. Over time, its applications expanded beyond the medical domain, finding relevance in various disciplines such as computer graphics and scientific visualization. Its flexibility and adaptability have made it an indispensable instrument for researchers and developers attempting to effectively visualize complex 3D data.

Four essential stages comprise the algorithm for marching cubes: space division, cell identification, border creation, and surface generation. In the first stage of the algorithm, space division, the virtual space is divided into a grid. A more refined grid subdivision improves the model's resolution. In the second phase, cell identification, the algorithm differentiates between cells containing the object and vacant cells. In the third stage, border creation, the system evaluates the vertices of cells along the border. Through linear interpolation, a smooth border is generated around the object. In the final phase, surface generation, the algorithm "marches" through the

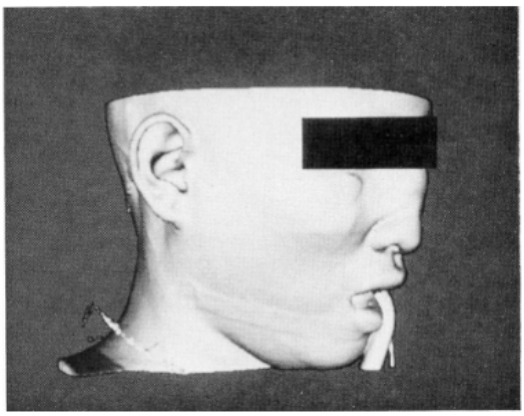

Figure 4.21: A 3D medical model, created with the marching cubes algorithm [91].

"cube" (cell grids) and creates triangular faces by connecting vertices derived from the cell grid or the boundary.

In a CFD simulator, it is possible to omit the first two stages (namely, space division and cell identification) of the marching cubes method. Given that the CFD simulator functions inside a grid, it is unnecessary for the rendering function to create an additional grid. Moreover, the fluid simulator already holds knowledge about the cells that contain fluid, hence making the cell identification process unnecessary. The possibility of omitting the first two stages of the marching cubes algorithm in a CFD simulator is what makes this algorithm so appealing.

The boundary definition stage in the marching cubes method is of significant importance in the handling of point cloud collections. In datasets of this kind, it is uncommon for individual data points to exhibit complete alignment with the vertices of the grid. Hence, it is essential to include the boundary defining stage in order to faithfully depict the underlying 3D structures, as seen in Figure 4.22 a). Nevertheless, in the context of a CFD simulator, the inclusion of this stage may be considered rather optional. In CFD simulations, each cell is classified as either a fluid cell or an empty cell[5]. Consequently, the boundary of the simulation domain will consistently coincide precisely with the grid, as seen in Figure 4.22 b). There are two reasons for preserving this step. The first, and most important, this step is responsible for identifying the border vertices. The second lies in its capacity to efficiently reduce boundary irregularities without needing to increase the grid resolution. This process involves a systematic traversal of the boundary, in which the program selects the four border points closest to the point in study. Subsequently, a set of linear interpolation is used, which takes into account the distances from the

[5]The density parameter is only used to determine the quality of the weld, not being synonymous with the quantity of fluid in the cell. Consequently, if the density at a given cell is greater than zero, that cell is designated as a fluid cell. A low density merely indicates that the cell contains numerous pores, resulting in a poorer quality.

central point to the others. The interpolations modify the position of the central point, leading to the smoothing of the curve, as seen in Figure 4.22 c). As a result, it is evident from Figure 4.22 d) that, even when using grids with lower resolutions, this process has the ability to convert rough meshes into more refined and visually appealing objects.

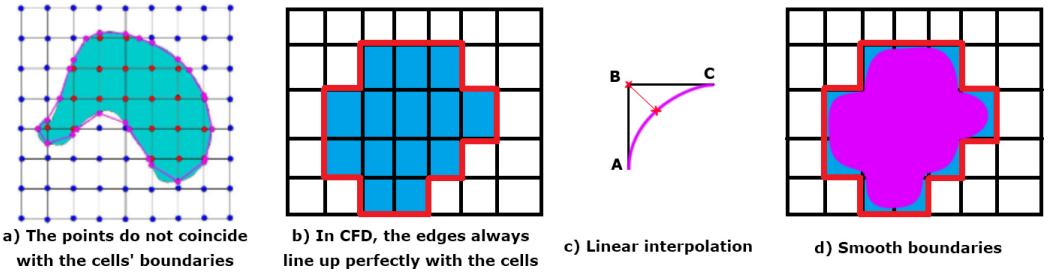

Figure 4.22: Boundary definition stage in marching cubes.

The concluding stage of the marching cubes algorithm is the phase that bestows the method with its designated name. During this phase, the system "marches" through the "cubes" (grid) constructing the mesh of the object. This step is also the most complex because it requires connecting the border vertices in the correct order to generate the faces accurately. Lorensen and Cline [91] highlighted that there were 2^8, or 256, potential methods for connecting the vertices inside each grid cell. This would have proven to be a highly intricate and computationally intensive task. However, the authors discovered that by leveraging symmetries and rotations, they could reduce the problem from 256 cases to 14 unique patterns. A dictionary was constructed with all the 14 distinct patterns, hence facilitating the identification of the specific pattern that matches to the cell being examined. Figure 4.23 displays these 14 patterns for reference.

4.4 Parallel Processing: Enhancing Computational Efficiency through GPU Integration

As stated before, the process of creating a fluid simulator requires significant computer resources. The process of dynamically generating the grid, solving the fluid equations, and rendering the fluid, all require traversing a substantial number of cells in order to attain the intended outcomes. Therefore, it is crucial to utilize the parallel processing capabilities of the Graphics Processing Unit (GPU) in order to optimize system performance.

In the Unity software framework, there exist two prominent methodologies which enable the use of GPU capabilities: vertex or fragment shaders [92] and compute shaders [93]. The primary distinction between these two programs lies in the fact that graphics shaders only operate with mesh or texture data, while compute shaders

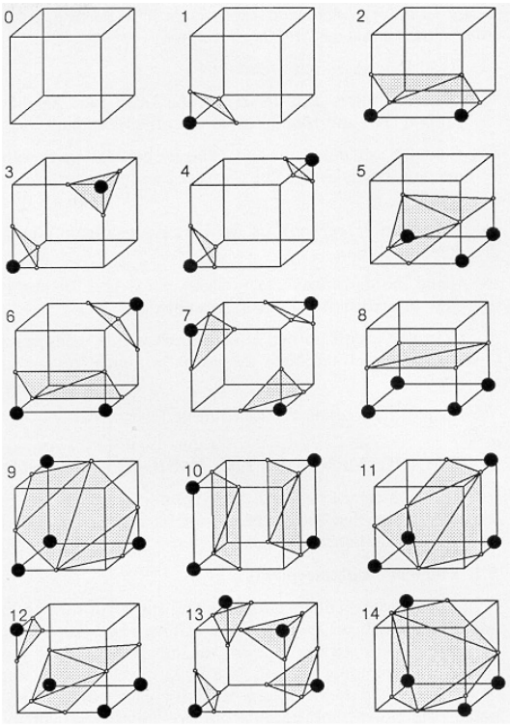

Figure 4.23: The 14 unique patterns of the marching cubes algorithm [91].

have the capability to operate with both mesh and texture data and data buffers. Due to this differentiation, graphics shaders are mostly used to oversee the rendering procedure of entities, assuming a pivotal function in addressing shading, texturing, and visual improvements during the rendering process. In contrast, compute shaders refer to specialized programs that are specifically designed for the purpose of massive parallelization of math operations. Compute shaders provide substantial value across a wide spectrum of computational activities, beyond their traditional affiliation with graphics-related operations.

In the given project's context, compute shaders emerge as the optimal selection for dynamically creating the grid, calculating the fluid equations, and drawing the fluid. This preference arises from the fact that most of the data is stored in vectors, and the need for a large number of calculations.

The best way to understand the working of the compute shaders is to look at Unity's example program, listed bellow.

```
1 #pragma kernel CSMain
2
3 RWTexture2D<float4> Result;
4
5 [numthreads(8,8,1)]
6 void CSMain (uint3 id : SV_DispatchThreadID)
```

```
7 {
8     Result[id.xy] = float4(id.x & id.y, (id.x & 15)/15.0, (id.y &
          15)/15.0, 0.0);
9 }
```

Every compute shader file contains at least one kernel, listed at the beginning of the file. These kernels serve as entry points for the program. Since a compute shader file can contain multiple kernels, they must be well-defined because the CPU needs to know the kernel number to invoke them correctly. Line 3 declares a global variable to store the data processed by the kernel. This line specifies a Two-Dimensional (2D) texture that can be both read from and written to, with each pixel containing a vector storing four floats. However, in this project, data buffers are predominantly used instead of textures. These can be declared as: `RWStructuredBuffer<cell> gridData;`. In this example, which is employed in the fluid compute shader, a buffer is created to hold a collection of structures of type `cell`. Following the code, the line `[numthreads(8,8,1)]` defines the dimensions of the thread groups created by the GPU. In this instance, each thread group resembles an 8x8 matrix, totaling 64 threads. Determining the optimal size for thread groups largely depends on the target hardware and the specific task at hand. In this project, since the data is stored in one-dimensional arrays, the thread groups have been set to 32x1x1. The remaining part of the compute shader code closely resembles a standard C# script, with the variable `id` representing the thread number.

Compute shaders are executed by the CPU through a C# script. During script initialization, the system identifies all the required kernels and stores their identifiers as integers. This process can be done as follows: `k_Advect = computeShader.FindKernel("Advect");`. Whenever a function requires the GPU to perform a task, it first needs to set up the necessary textures or buffers for the kernel. This setup involves creating a texture or a compute buffer and then writing data to it. After preparing the buffer, the script proceeds to assign it to the kernel that will be called. Following that, the system dispatches the required kernel using the identification number found at the beginning of the script. Once the dispatch is complete, the CPU waits for the GPU's response. The final step involves retrieving the data from the buffer returned by the GPU. Below is the C# code used to call the advection kernel.

```
1 private void GPU_Advect()
2 {
3     ComputeBuffer buff_gridData = new ComputeBuffer(nCells, 68);
4
5     cell[] input = grid.ToArray();
```

```
6       cell[] output = new cell[nCells];
7
8       buff_gridData.SetData(input);
9
10      computeShader.SetBuffer(k_Update, "gridData", buff_gridData);
11      computeShader.SetBuffer(k_Advect, "gridData", buff_gridData);
12
13      computeShader.SetInt("nCells", nCells);
14      computeShader.SetFloat("deltaTime", Time.deltaTime);
15
16      computeShader.Dispatch(k_Update, nCells, 1, 1);
17      computeShader.Dispatch(k_Advect, nCells, 1, 1);
18
19      buff_gridData.GetData(output);
20      buff_gridData.Release();
21
22      grid.Clear();
23      grid.AddRange(output);
24  }
```

In this project parallel processing was applied to the dynamic grid creation and to solving the Navier-Stokes equations. In particular, for the *diffusion*, the *advection* and *projection* steps.

4.5 System Overview

The purpose of this section is to link the previous sections, presenting how the system works as a whole.

This project operates in two environments, the real world and the virtual world. As presented in the first section of this chapter, these worlds are connected via the HTC Vive Pro 2. This set of equipment is capable of reading the user's position and inputs in the real world. On the other hand, it provides the user with images, sounds and tactile feedback from the virtual world.

The virtual world consists of an avatar of the user, props (workbenches and other objects that the user cannot move), tools that the user can interact with and the welding simulator. In this world, the position and rotation of the user's hands and head, as well as their inputs, are provided to the tools. In turn, the tools can interact with each other. The cutting pliers communicate with the torch if the user wants to cut the excess wire. The torch sends a signal to the mask, which determines whether a weld is being made or not, to simulate the opening and closing of the mask's glass. In addition, the torch provides its position to the welding simulator, so that the dynamic grid is generated in the proper place. Within the welding simulator, the grid functions as a central storage hub for the fluid state. At the beginning of each iteration, data is sent to the *diffusion* function, which subsequently passes it on to

the *advection* and finally to the *projection*. At the end, the updated fluid data is once again sent to the grid for storage. Additionally, it is dispatched to the fluid rendering function.

Figure 4.24 displays the whole system as well as the relationships between its components.

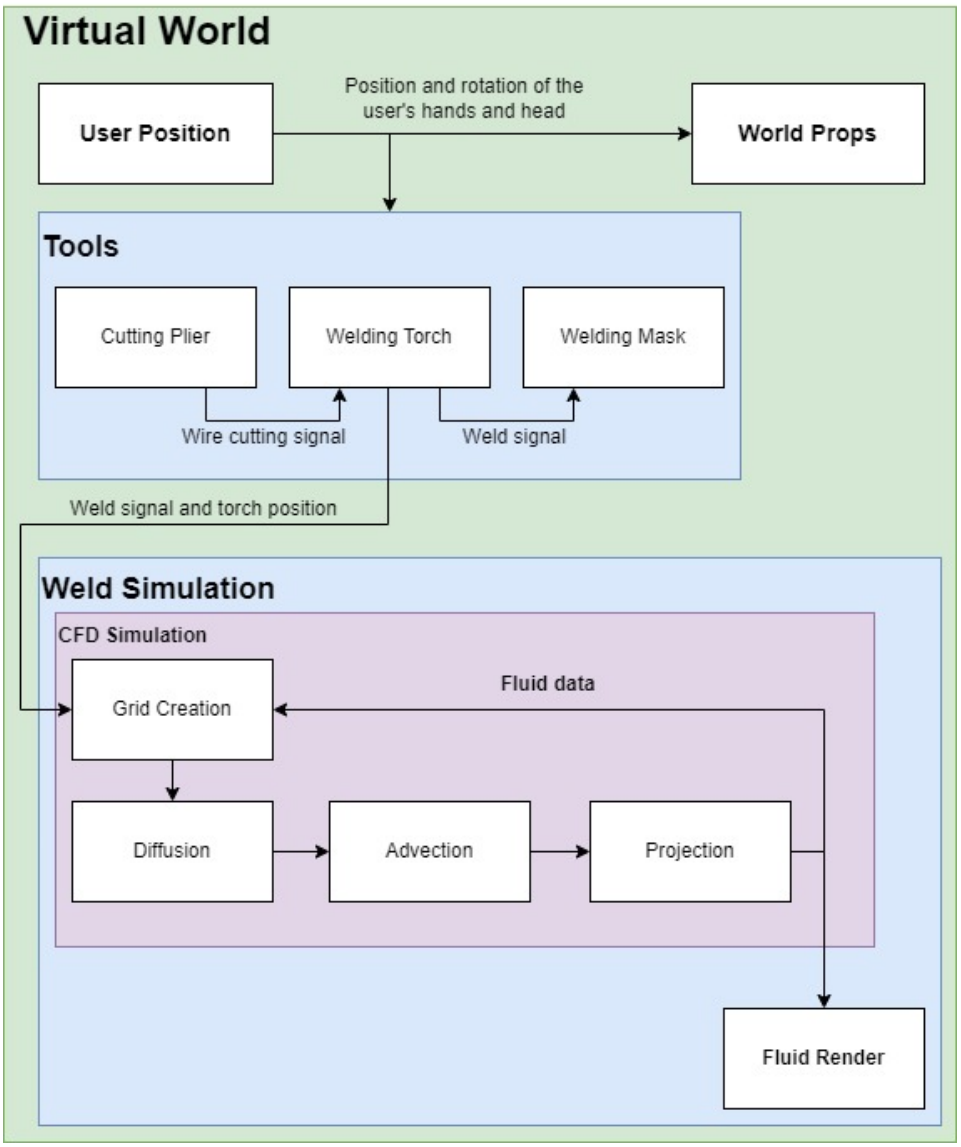

Figure 4.24: Diagram of the complete system and the relationships between its elements.

Chapter 5

Conclusion

The conclusion chapter offers a comprehensive summary of the research conducted and work developed in this project. It concludes by highlighting potential areas that may be further improved and developed.

5.1 Work Developed

Through this research, this project developed a classification system for evaluating and comparing welding simulators, which will assist in identifying the essential characteristics that should be included in each level of classification. By doing so, it will provide a useful resource for both researchers and instructors in the welding field, to better assess and select the most appropriate simulators for their needs and to promote the development of more effective and efficient simulators in the future.

The work conducted produced some promising results but also highlighted areas that require further development. In the field of VR, as demonstrated in Chapter 4, this project proved to be successful in accurately capturing user movements using the HTC VIVE Pro 2. Furthermore, it effectively implemented tools such as the welding torch, cutting pliers, and welding mask, which users could freely interact with and utilize. Additionally, the project successfully implemented a tracker that could be attached to a real welding torch, replacing the traditional VR controller.

Regarding the welding simulation, it was decided to implement a fluid simulator to accurately replicate the welding process. This step consumed a significant amount of time since it was the most complex aspect of the project. The initial

iteration implemented a Smoothed-Particle Hydrodynamics (SPH) simulator. This simulator has proved capable of creating horizontal welds and correctly conveying the temperature of the material. However, it had problems creating vertical welds, as it was unable to support itself, and always fell to the bottom, this is depict in Figure 5.1. In addition, the visual quality of the material was poor. This could be compensated for by decreasing the particle size, which in turn would lead to an increase in the number of particles and the computational cost. This was the point that proved to be the most disadvantageous in SPH. Its high number of particles resulted in simulations of less than 10 FPS, breaking the sense of immersion[1].

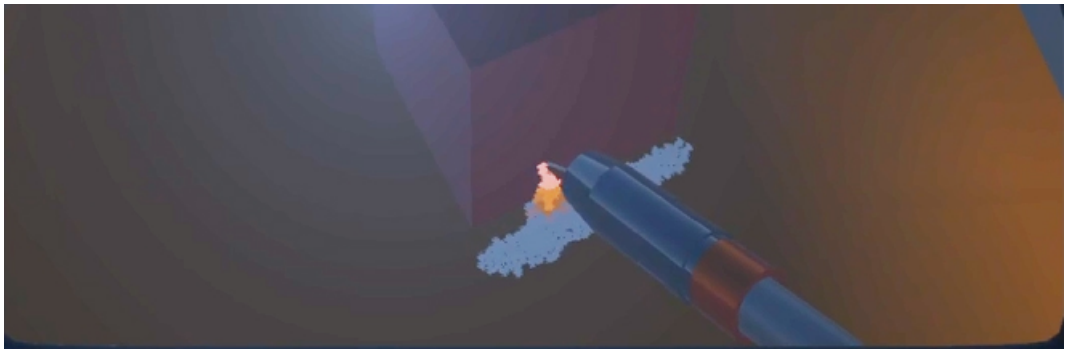

Figure 5.1: SPH flaws: The material is incapable of sustaining itself.

The second approach involved the implementation of a Computational Fluid Dynamics (CFD) simulator. This type of simulator is renowned for its versatility and the ability to simulate a wide range of fluid scenarios, including heat transfer phenomena, offering a high level of accuracy in capturing complex fluid behaviors. The project successfully implemented a CFD simulator with a static grid. Figure 5.2 shows the simulation CFD implemented on a static grid. In this simulation, a force is applied in the middle of the grid, which extends outwards in all directions. As can be seen, the fluid particles form a sphere, which ends up colliding with the grid walls. However, from this test, it became evident that the low frame rate remained an issue. For a grid with 15625 cells (25 by 25 by 25) the average frame rate was 13,5 FPS. The same issue may be found in other tests, such as the one seen in the video at [94]. To address this problem, a dynamic grid strategy was employed. The improvement in implementing a dynamic grid compared to a static grid is not direct, since for the same number of cells both perform equally. However, the dynamic grid has the advantage of only existing at the points where the user welds, drastically reducing the number of cells. The biggest setback with the dynamic grid was the drastic drop (between 10 and 20 FPS) every time new cells were created. However, after implementing the function responsible for creating the grid in the GPU, these FPS drops disappeared.

[1] As a point of reference, in order to maintain the sense of immersion, the simulator must run at a minimum of 30fps [57].

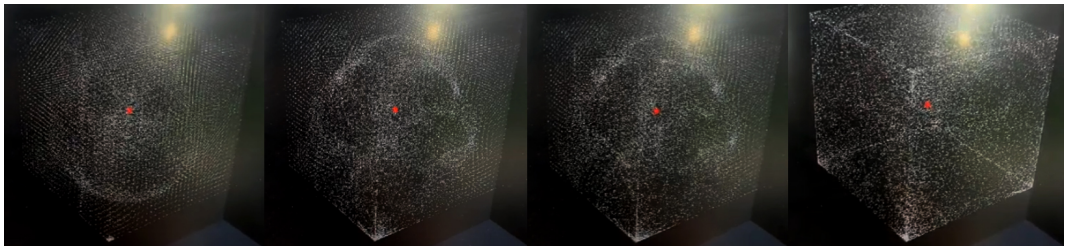

Figure 5.2: Implemented CFD simulation in a static grid (video available at [95]).

To further improve the simulator, the next step involved leveraging the parallel processing capabilities of the GPU to compute the Navier-Stokes equations. While the *diffusion* and *advection* steps were successfully implemented, the *projection* step proved to be challenging and could not be fully realized. The inability to implement the *projection* function hindered the project's progress, as it consumed the time needed to implement fluid rendering. However, of the two functions implemented, there has been a great improvement. To carry out these tests, two versions of the simulator were used, one with the CPU functions and the other with the GPU functions. Each function was then tested individually for rectangular grid with 10000 cells. The diffusion function showed an average improvement of 41,3 FPS. For the advection function, there was a greater increase, around 126,8 FPS. This increase is justified by the number of calculations needed to determine Q_0 and the weight of the neighbours, which can now be carried out in parallel.

The present study effectively tackles the three fundamental scientific inquiries that form the basis for the advancement of virtual reality welding simulators.

Scientific Question 1: *How can the intricacies of welding's physical nature be accurately reproduced within the context of a virtual reality simulation?*

A fluid simulator has been determined to be the most effective method for simulating the weld. According to the exhaustive analysis. Computational Fluid Dynamics (CFD) simulators have become the preferred option owing to their remarkable accuracy in simulating the behavior of fluids. It is important to mention that the initial experiments were conducted using Smoothed-Particle Hydrodynamics (SPH) simulators. Nonetheless, the inability of these methods to produce genuine outcomes necessitated the shift towards simulations based on CFD.

Scientific Question 2: *In what systematic ways can virtual reality welding simulators be classified and evaluated?*

Scientific Question 3: *In the context of welding simulators, which fundamental characteristics define an appropriate balance between cost and quality?*

These two questions are intricately interwoven, and this investigation has revealed a unified solution. In order to resolve both inquiries, the implementation of a comprehensive classification system has been demonstrated to be indispensable. By

formulating a methodical structure for assessing virtual reality welding simulators, it was utilized an instrument that not only facilitates methodical classification but also establishes a foundation for determining the simulators' cost-effectiveness and quality. By utilizing this framework, decision-makers are granted the ability to evaluate the qualities that are most significant in relation to their particular welding needs.

In summary, the project successfully developed a classification system for evaluating and comparing welding simulators. Furthermore, it implemented a virtual reality environment and tools for the user to interact with. It was also effective at translating the user motion from the actual world to the virtual one. However, the welding simulation presented mixed results. The SPH simulation proved capable of creating horizontal welds and correctly conveying the temperature of the material, but it faild in simulating vertical welds. Furthermore, it showed a low resolution and frame rate. The CFD simulation with a static grid exhibited good fluid dynamics but also suffered from low frame rates. The same architecture, but with a dynamic grid, proved especially beneficial after the implementation on the GPU, since it eliminated FPS drops when generating new grid cells. In addition, the implementation of the solvers for the Navier-Stokes equations on the GPU showed strong improvements. However, the implementation of the *projection* function has not been finalised. The formulation of a classification system and the provision of exhaustive responses to the scientific inquiries usher in a paradigm shift in virtual reality welding simulation. Providing researchers with enhanced capabilities to develop, assess, and optimize these simulators, thereby promoting progress in industrial and academic welding methodologies.

5.2 Future Work

As time progresses, there is always room for improvement. In this project, the developed classification system can be further enhanced and should be regularly updated to incorporate new techniques and resources emerging in the fields of virtual reality and welding. Regarding the virtual environment, there is significant potential for improvement. This includes refining graphics for a more realistic experience and implementing more user-friendly interactions. In the realm of welding, the system can be enhanced by incorporating additional welding positions and techniques. With advancements in artificial intelligence, it would be advantageous to introduce a virtual coaching system and tools for evaluating user performance. Lastly, concerning the weld simulation, it is imperative to complete the implementation of the CFD simulator and integrate the fluid rendering functions.

References

[1] H.-S. Lee, "10 - diffusion bonding of metal alloys in aerospace and other applications," in *Welding and Joining of Aerospace Materials* (M. Chaturvedi, ed.), Woodhead Publishing Series in Welding and Other Joining Technologies, pp. 305–327, Woodhead Publishing, second edition ed., 2021. [Cited on page 1]

[2] M. E. Mfg, *Welding and the World of Metals*. Miller Electric Mfg, first ed., 1962. [Cited on pages 1, 2, and 3]

[3] K. Weman, *Welding Processes Handbook*. Woodhead Publishing Series in Welding and Other Joining Technologies, Woodhead Publishing Limited, 2nd edition ed., November 2011. [Cited on pages 1, 2, 3, 16, and 17]

[4] M. Russell, "Welding torch." `https://patents.google.com/patent/US2274631A/en`, March 1942. Last accessed on 30/03/2023. [Cited on page 2]

[5] J. Mcgrath, I. Mandl, and J. Pacolet, "Report on labour shortages and surpluses," tech. rep., European Labour Authority, November 2021. Last accessed on 30/03/2023. [Cited on page 3]

[6] V. S. Chan, H. N. H. Haron, M. I. B. M. Isham, and F. B. Mohamed, "VR and AR virtual welding for psychomotor skills: a systematic review," *Multimedia Tools and Applications*, vol. 81, pp. 12459–12493, April 2022. doi: `10.1007/s11042-022-12293-5`. [Cited on pages 3, 4, 6, 12, 22, 23, 33, 34, 35, and 41]

[7] K. Miller and C. Petti, "Teaching welding: An overview of classroom methods," *Welding Journal*, vol. 93, no. 10, pp. 35–40, 2014. [Cited on page 4]

[8] J. Sacks, "Teaching welding in a hands-on environment," *The Fabricator*, 2016. Last accessed on 30/03/2023. [Cited on page 4]

[9] Health and Safety Executive, "Welding: Health risks from welding - HSE." `https://www.hse.gov.uk/welding/health-risks-welding.htm`, August 2021. Last accessed on 13/01/2023. [Cited on pages 4 and 5]

[10] B. Smith and P. Schuette, "Virtual and augmented reality welding training," *Welding Journal*, vol. 97, no. 2, pp. 45–49, 2018. [Cited on page 6]

[11] Q. Wang, Y. Cheng, W. Jiao, M. T. Johnson, and Y. Zhang, "Virtual reality human-robot collaborative welding: A case study of weaving gas tungsten arc welding," *Journal of Manufacturing Processes*, vol. 48, pp. 210–217, 2019. [Cited on page 6]

[12] P. Milgram and F. Kishino, "A taxonomy of mixed reality visual displays," *IEICE TRANSACTIONS on Information and Systems*, vol. 77, no. 12, pp. 1321–1329, 1994. [Cited on pages 11 and 12]

[13] I. D. Foundation, "Virtuality continuum." `https://www.interaction-design.org/literature/topics/virtuality-continuum`. Last accessed on 05/01/2023. [Cited on page 12]

[14] G. de Moura Costa, M. R. Petry, and A. P. Moreira, "Augmented reality for human-robot collaboration and cooperation in industrial applications: A systematic literature review," *Sensors*, vol. 22, no. 7, 2022. [Cited on pages 12 and 13]

[15] M. J. Maas and J. M. Hughes, "Virtual, augmented and mixed reality in k–12 education: a review of the literature," *Technology, Pedagogy and Education*, vol. 29, no. 2, pp. 231–249, 2020. [Cited on pages 12 and 13]

[16] L. Muñoz-Saavedra, L. Miró-Amarante, and M. Domínguez-Morales, "Augmented and virtual reality evolution and future tendency," *Applied Sciences*, vol. 10, no. 1, 2020. [Cited on pages 12 and 13]

[17] H. Kato and M. Billinghurst, "Marker tracking and hmd calibration for a video-based augmented reality conferencing system," in *Proceedings IEEE and ACM International Workshop on Augmented Reality (IWAR'99)*, pp. 85–94, 1999. [Cited on page 12]

[18] R. T. Azuma, "Recent advances in augmented reality," *IEEE computer graphics and applications*, vol. 21, no. 6, pp. 34–47, 2001. [Cited on page 12]

[19] Q. Li and G. Li, "Augmented reality technology and its applications in education," *Journal of Computers in Education*, vol. 4, no. 4, pp. 435–448, 2017. [Cited on page 12]

[20] L. Zhou and D. Dredge, "Augmented reality in tourism and hospitality: A literature review," *Journal of Travel Research*, vol. 57, no. 7, pp. 803–825, 2018. Last accessed on 30/03/2023. [Cited on page 12]

[21] M. U. Khan, S. Khan, and M. A. Khan, "Augmented reality marketing: Consumer preferences and attitudes," *Journal of Business Research*, vol. 89, pp. 35–44, 2018. [Cited on page 12]

[22] F. Muñoz-Leiva, J. Sánchez-Fernández, and F. J. Montoro-Ríos, "Augmented reality: A promising tool for enhancing consumer engagement and experiences in marketing," *Journal of Business Research*, vol. 100, pp. 486–495, 2019. [Cited on page 12]

[23] K. Ozcan, M. Ozel, and G. Okten, "A review of augmented reality applications in construction: Opportunities and challenges," in *2019 27th Signal Processing and Communications Applications Conference (SIU)*, pp. 1–4, IEEE, 2019. [Cited on pages 12 and 13]

[24] R. T. Azuma, G. Bishop, S. Neely, and T. Miyasato, "Tracking in unprepared environments for augmented reality systems," in *Proceedings of the 2nd IEEE/ACM International Symposium on Mixed and Augmented Reality*, pp. 36–45, 2005. [Cited on page 12]

[25] F. Wen, Q. Li, Y. Huang, and Z. Li, "Privacy concerns and issues in augmented reality applications," *International Journal of Communication Systems*, vol. 31, no. 10, 2018. [Cited on page 12]

[26] G. Riva, "Applications of virtual environments in medicine," *Methods of information in medicine*, vol. 42, no. 05, pp. 524–534, 2003. [Cited on page 13]

[27] S. Behmadi, F. Asadi, M. Okhovati, and R. E. Sarabi, "Virtual reality-based medical education versus lecture-based method in teaching start triage lessons in emergency medical students: Virtual reality in medical education," *Journal of advances in medical education & professionalism*, vol. 10, pp. 48–53, January 2022. [Cited on page 13]

[28] M. Moshell, C. Hugues, and R. B. Loftin, *Virtual Reality as a Tool for Academic Learning*. Lawrence Erlbaum Associates, 2002. [Cited on page 13]

[29] A. Burova, P. B. Palma, P. Truong, J. Mäkelä, H. Heinonen, J. Hakulinen, K. Ronkainen, R. Raisamo, M. Turunen, and S. Siltanen, "Distributed asymmetric virtual reality in industrial context: Enhancing the collaboration of geographically dispersed teams in the pipeline of maintenance method development and technical documentation creation," *Applied Sciences*, vol. 12, no. 8, 2022. [Cited on page 13]

[30] J. Rickel, S. Marsella, J. Gratch, R. Hill, D. Traum, and W. Swartout, "Toward a new generation of virtual humans for interactive experiences," *IEEE Intelligent Systems*, vol. 17, no. 4, pp. 32–38, 2002. [Cited on page 13]

[31] D. Harris, T. Arthur, J. Kearse, M. Olonilua, E. Hassan, T. de Burgh, M. Wilson, and S. J. Vine, "A comparison of live fire, 2d video, and virtual reality simulations for judgemental training in the military," 2022. [Cited on page 13]

[32] J. Hou, X. R. Li, and Y. Li, "Virtual reality and mixed reality for virtual learning environments," *Educational Technology & Society*, vol. 21, no. 4, pp. 1–15, 2018. [Cited on page 13]

[33] D. A. Bowman, R. P. McMahan, and E. D. Ragan, "Virtual reality: How much immersion is enough?," *Computer*, vol. 51, no. 6, pp. 25–31, 2018. [Cited on page 13]

[34] Y. Chang, H. Kim, and W. Woo, "Survey of virtual reality technologies, applications, and challenges," *Symmetry*, vol. 13, no. 3, 2021. [Cited on page 14]

[35] Oculus, "Oculus rift s." `https://www.oculus.com/rift-s/`, 2023. Last accessed on 08/09/2023. [Cited on page 14]

[36] HTC, "Htc vive pro 2 full kit." `https://www.vive.com/us/product/vive-pro2-full-kit/overview/`, 2023. Last accessed on 08/09/2023. [Cited on page 14]

[37] Sony, "Playstation vr." `https://www.playstation.com/pt-pt/ps-vr/`, 2023. Last accessed on 08/09/2023. [Cited on page 15]

[38] V. Corporation, "Valve index." `https://store.steampowered.com/sub/354231/`, 2023. Last accessed on 08/09/2023. [Cited on page 15]

[39] R. to VR, "Samsung odyssey vr headset: Windows mixed reality now available—everything you need to know." `https://www.roadtovr.com/samsung-odyssey-vr-headset-mixed-reality-now-available-everything-you-need-to-know/`, 2023. Last accessed on 08/09/2023. [Cited on pages 15 and 16]

[40] HP, "Hp reverb g2 vr headset." `https://www.hp.com/pt-pt/vr/reverb-g2-vr-headset.html`, 2023. Last accessed on 08/09/2023. [Cited on pages 15 and 16]

[41] T. W. Institute, "What is welding? - Definition, processes and types of welds." `https://www.twi-global.com/technical-knowledge/faqs/what-is-welding`, 2023. Last accessed on 01/03/2023. [Cited on page 16]

[42] A. W. Society, *Welding Handbook, 9th edition, Volume 1: Welding Science and Technology*. Miami, Florida: American Welding Society, 2001. [Cited on pages 17, 22, and 29]

[43] J. Worman, "What is the best welding process?," *The National Board of Boiler and Pressure Vessel Inspectors*, 2017. Last accessed on 01/03/2023. [Cited on pages 17, 18, 19, and 20]

[44] WeldGuru, "Welding processes: An in-depth look at mig, tig, stick, and more." `https://weldguru.com/welding-processes/`, 2021. Last accessed on 12/03/2023. [Cited on pages 17, 18, 19, 20, 21, and 22]

[45] A. W. Society, "Shielded metal arc welding (SMAW)." https://awo.aws.org/glossary/shielded-metal-arc-welding-smaw, 2021. Last accessed on 12/03/2023. [Cited on page 18]

[46] A. W. Society, "Gas tungsten arc welding (GTAW)." https://awo.aws.org/glossary/gas-tungsten-arc-welding-gtaw/. Last accessed on 12/03/2023. [Cited on page 19]

[47] Fractory, "Mig welding explained: Understanding the basics." https://fractory.com/mig-welding-explained/, 2021. Last accessed on 12/03/2023. [Cited on page 20]

[48] American Welding Society, "Gas metal arc welding (gmaw)." https://awo.aws.org/glossary/gas-metal-arc-welding-gmaw/. Last accessed on 13/03/2023. [Cited on pages 20 and 21]

[49] WeldGuru, "Mig welding." https://weldguru.com/mig-welding/, September 2022. Last accessed on 03/03/2023. [Cited on pages 20 and 21]

[50] W. Welders, "Mig welding for beginners: A comprehensive guide." https://waterwelders.com/mig-welding-for-beginners/, 2022. Last accessed on 12/03/2023. [Cited on page 21]

[51] S. Sild, "Mig welding explained." https://fractory.com/mig-welding-explained/, April 2022. Last accessed on 05/03/2023. [Cited on page 20]

[52] "Aws d1.1/d1.1m:2020 structural welding code - steel," 2020. [Cited on page 22]

[53] International Organization for Standardization, "ISO 6947:2019 welds – working positions – definitions of angles of slope and rotation." https://www.iso.org/standard/74316.html, 2019. Last accessed on 30/03/2023. [Cited on page 22]

[54] American Welding Society, "ANSI/AWS a2.4 standard symbols for welding, brazing, and nondestructive examination." https://pubs.aws.org/p/1999/a242020-standard-symbols-for-welding-brazing-and-nondestructive-examination, 2020. Last accessed on 30/03/2023. [Cited on page 22]

[55] Millers Electric Mfg. Co Training Department, "Intro to welding 8 - welding joint types positions and symbols." https://www.millerwelds.com/Training/PresentationsQuizzes/IntroToWelding/Welding8/presentation_html5.html, 2016. Last accessed on 01/02/2023. [Cited on page 22]

[56] E. R. Bohnart, *Welding: Principles and Practices*. McGraw-Hill, 5th ed., 2018. [Cited on page 22]

[57] M. J. Harris, *Fast Fluid Dynamics Simulation on the GPU*, ch. 38, pp. 845–866. NVIDIA Corporation, 2007. [Cited on pages 24, 52, 55, 56, 58, 63, and 72]

[58] S. Sommavilla, "Smoothed particle hydrodynamics: A guided journey into the basics of the sph method." `https://www.dive-solutions.de/blog/sph-basics`, December 2020. Last accessed on 28/08/2023. [Cited on pages 24 and 25]

[59] D. Violeau, *Fluid mechanics and the SPH method: theory and applications*. Oxford University Press, 2012. [Cited on page 25]

[60] K. Kumar, Q. Wang, and R. Hosseini, "Research - lattice boltzmann method." `https://www.geoelements.org/research/lbm/`, 2023. Last accessed on 15/08/2023. [Cited on pages 25 and 26]

[61] J. D. Anderson and J. Wendt, *Computational fluid dynamics*, vol. 206. Springer, 1995. [Cited on page 27]

[62] S. H. Roosta, *Parallel processing and parallel algorithms: theory and computation*. Springer Science & Business Media, 2012. [Cited on page 28]

[63] R. T. Stone, K. P. Watts, P. Zhong, and C.-S. Wei, "Physical and cognitive effects of virtual reality integrated training," *Human Factors*, vol. 53, no. 5, pp. 558–572, 2011. [Cited on pages 31, 32, 34, 35, and 36]

[64] L. Da Dalto, F. Benus, and O. Balet, "The use and benefits of virtual reality tools for the welding training," in *63rd Annual Assembly & International Conference of the International Institute of Welding, Istanbul, Turkey*, 2010. [Cited on pages 32 and 37]

[65] M. E. M. LLC, "Educational resources and product guide." `MillerWelds.com`, 2022. Last accessed on 02/02/2023. [Cited on page 32]

[66] M. I. Mat Isham, H. N. Hj Haron, F. b. Mohamed, and C. V. Siang, "Vr welding kit: Accuracy comparison between smartphone vr and standalone vr using rmse," in *2021 IEEE International Conference on Computing (ICOCO)*, pp. 341–346, 2021. [Cited on page 36]

[67] C. Choquet, "Arc+: Today's virtual reality solution for welders," *Internet Page, Jan*, vol. 1, no. 6, 2008. [Cited on pages 37 and 38]

[68] Y. Ye, T. Zhou, and J. Du, "Robot-assisted immersive kinematic experience transfer for welding training," *Journal of Computing in Civil Engineering*, vol. 37, no. 2, 2023. [Cited on page 41]

[69] D. Beck, L. Morgado, and P. O'Shea, "Finding the gaps about uses of immersive learning environments: a survey of surveys," *Journal of Universal Computer Science*, vol. 26, pp. 1043–1073, 2020. [Cited on pages 41 and 42]

[70] M. Couto, "Vr welding simulator." `https://youtu.be/onqTmsQ_c2o?si=5z7126Jbneiupk3D`, 2023. [Video File] Last accessed on 17/10/2023. [Cited on page 49]

[71] HTC Corporation, *HTC VIVE Tracker (3.0) Developer Guidelines v1.0*, January 2021. [Cited on page 50]

[72] U. Technologies, "Unity rigidbody documentation." `https://docs.unity3d.com/ScriptReference/Rigidbody.html`, 2023. Last accessed on 19/09/2023. [Cited on page 52]

[73] M. Fowler, "Stokes' law." `https://galileo.phys.virginia.edu/classes/152.mf1i.spring02/Stokes_Law.htm`, 2002. Last accessed on 08/09/2023. [Cited on page 52]

[74] I. Alduán and M. A. Otaduy, "Sph granular flow with friction and cohesion," SCA '11, (New York, NY, USA), p. 25–32, Association for Computing Machinery, 2011. [Cited on page 52]

[75] M. Couto, "Sph - testing weld creation 1." `https://youtu.be/3Y6C_Ytz89g?si=8X2V8bNwmIw0NF7U`, 2023. [Video File] Acesso em 17/10/2023. [Cited on page 52]

[76] M. Couto, "Sph - testing weld creation 2." `https://youtu.be/W-x-jysQ83w?si=dYtL4FH-makwSauS`, 2023. [Video File] Acesso em 17/10/2023. [Cited on page 52]

[77] M. Couto, "Cfd - dynamic grid generation." `https://youtu.be/M0fcmWJKy68?si=MnJrKcI0J5j1wGWM`, 2023. [Video File] Acesso em 17/10/2023. [Cited on page 55]

[78] J. Stam, "Real-time fluid dynamics for games," in *Proceedings of the Game Developer Conference*, March 2003. [Cited on pages 55 and 56]

[79] E. Larionov, C. Batty, and R. Bridson, "Variational stokes: A unified pressure-viscosity solver for accurate viscous liquids," *ACM Trans. Graph.*, vol. 36, July 2017. [Cited on page 56]

[80] H. Su, T. Xue, C. Han, C. Jiang, and M. Aanjaneeya, "A unified second-order accurate in time mpm formulation for simulating viscoelastic liquids with phase change," *ACM Transactions on Graphics*, vol. 40, p. 119, August 2021. [Cited on page 56]

[81] J. Panuelos, R. Goldade, and C. Batty, "Efficient Unified Stokes using a Polynomial Reduced Fluid Model," in *Eurographics/ ACM SIGGRAPH Symposium*

on Computer Animation - Posters (D. L. Michels, ed.), The Eurographics Association, 2020. [Cited on page 56]

[82] M. Couto, "Cfd - density function test." `https://youtu.be/QRZmnKWFIhU?si=OtEfnTOHeNfPPlgE`, 2023. [Video File] Acesso em 17/10/2023. [Cited on page 57]

[83] J. Stam, "Stable fluids," in *Proceedings of SIGGRAPH*, 1999. [Cited on pages 57 and 61]

[84] M. Couto, "Cfd - advection function test." `https://youtu.be/N7fFRpA190I?si=X8JVDOz8rPFbXYg0`, 2023. [Video File] Acesso em 17/10/2023. [Cited on page 60]

[85] J. Bolz, I. Farmer, E. Grinspun, and P. Schröder, "Sparse matrix solvers on the gpu: Conjugate gradients and multigrid," in *Proceedings of SIGGRAPH*, 2003. [Cited on page 63]

[86] N. Goodnight, C. Woolley, G. Lewin, D. Luebke, and G. Humphreys, "A multigrid solver for boundary value problems using programmable graphics hardware," in *Proceedings of the SIGGRAPH/Eurographics Workshop on Graphics Hardware*, 2003. [Cited on page 63]

[87] J. Krüger and R. Westermann, "Linear algebra operators for gpu implementation of numerical algorithms," in *Proceedings of SIGGRAPH*, 2003. [Cited on page 63]

[88] G. R. Morris and V. K. Prasanna, "An fpga-based floating-point jacobi iterative solver," in *8th International Symposium on Parallel Architectures, Algorithms and Networks (ISPAN'05)*, pp. 8–pp, IEEE, 2005. [Cited on page 63]

[89] S. Green, "Screen space fluid rendering for games." `https://developer.download.nvidia.com/presentations/2010/gdc/Direct3D_Effects.pdf`, March 2010. [Cited on page 64]

[90] N. Amenta, M. Bern, and M. Kamvysselis, "A new voronoi-based surface reconstruction algorithm," in *Proceedings of the 25th annual conference on Computer graphics and interactive techniques*, pp. 415–421, 1998. [Cited on page 64]

[91] W. E. Lorensen and H. E. Cline, "«*Marching cubes: A high resolution 3D surface construction algorithm*»," pp. 163–169, ACM Press, 1987. doi = 10.1145/37401.37422. [Cited on pages 64, 65, 66, and 67]

[92] U. Technologies, "Unity vertex and fragment shader documentation." `https://docs.unity3d.com/Manual/SL-VertexFragmentShaderExamples.html`, 2023. Last accessed on 18/09/2023. [Cited on page 66]

[93] U. Technologies, "Unity compute shader documentation." `https://docs.unity3d.com/Manual/class-ComputeShader.html`, 2023. Last accessed on 18/09/2023. [Cited on page 66]

[94] M. Couto, "Cfd - low performance when using only the cpu." `https://youtube.com/shorts/Ttk1PeixGNI?si=vhqUR3tRT30SXbQ1`, 2023. [Video File] Acesso em 17/10/2023. [Cited on page 72]

[95] M. Couto, "Cfd - static grid." `https://youtube.com/shorts/dK-MjFP83mM?si=db-eAJMM9UlE6xWZ`, 2023. [Video File] Acesso em 17/10/2023. [Cited on page 73]